AN ABSTRACT OF THE THESIS OF

Chun Chou for the degree of Master of Science

in Forest Products presented on June 5, 1984

Title: Effect of Drying on Damping and Stiffness of Nailed Joints between Wood and Plywood

Abstract approved: Redacted for Privacy

Dr. Anton Polensek

Wood components, usually assembled in green or semi-dry condition, dry during the initial service life. To evaluate the effect of such drying on joint stiffness and damping, cyclic-load tests were conducted on single-nail joints of wood and plywood that had been exposed to drying cycles. Additional effects studied were the surface condition of lumber and level of cyclic load. Tests showed that the stiffness decreased with load but remained the same for the planed and unplaned surface condition. The surface condition did affect the damping ratio when a tight interlayer contact existed. The effect of load level on damping ratio depended on the drying-produced gap between the lumber and plywood. The results show that the damping ratio and slip modulus were significantly smaller for joints with the gap than for those without it.

In a preliminary study the possibility was examined of using a free-vibration test for measuring the damping ratio of nailed joints. No simple arrangement could be devised for a reliable prediction of the ratio.

Effect of Drying on Damping and Stiffness of Nailed Joints between Wood and Plywood

by

Chun Chou

A THESIS

submitted to

Oregon State University

in partial fulfillment of
the requirements for the
degree of

Master of Science

Completed June 5, 1984

Commencement June 1985

APPROVED:

Redacted for Privacy

Professor of Forest Products in charge of major

Redacted for Privacy

Head of Department of Forest Products

Redacted for Privacy

Dean of Graduate School

Date thesis is presented June 5, 1984

Typed by Donna Lee Norvell-Race for Chun Chou

TABLE OF CONTENTS

I. INTRODUCTION 1

II. LITERATURE REVIEW. 4

2.1 Damping 4
2.1.1 Damping Sources in Wood Nailed Joint. . . 4
2.1.1.1 Material Damping 7
2.1.1.2 Frictional Damping at Contact Surfaces in Joints 10
2.1.2 Theoretical Concepts of Damping Evaluation. 14
2.1.2.1 Free-vibration Test. 14
2.1.2.2 Cyclic-load Test 22
2.2 Stiffness 25
2.3 Review of Pertinent Literature. 26

III. EXPERIMENTAL PROCEDURE 29

3.1 Procedure Selection 29
3.1.1 Preliminary Testing 29
3.1.2 Procedure Evaluation. 36
3.2 Materials and Methods 36
3.2.1 Material Selection and Specimen Construction. 36
3.2.2 Experimental Design 41
3.2.3 Testing Arrangement 44
3.2.4 Testing Procedure 45

IV. RESULTS AND DISCUSSION 48

4.1 Experimental Data 48
4.2 Data Reduction. 53
4.3 Data Analysis 55
4.3.1 Combined Effects of all Variables 55
4.3.2 Effect of MC. 57
4.3.3 Effect of Load Level. 64
4.3.4 Effect of Interface Roughness 74
4.4 Practical Impact and Application. 76

V. CONCLUSIONS AND RECOMMENDATIONS. 79

BIBLIOGRAPHY. 81

APPENDICES

A: Statistics for Variables Investigated 83
B: Properties and MC of Materials. 92

LIST OF FIGURES

Figure		Page
2.1	Free-vibration test of a beam.	5
2.2	True displacement of beam against time in free-vibration test.	6
2.3	Cross section of a typical nailed joint.	8
2.4	Hypothetical shape of deformation in the nailed joint.	9
2.5	Loading situation in slip damping.	12
2.6	Unloading situation in slip damping.	13
2.7	Single-degree-of-freedom system.	15
2.8	Time-displacement traces of one-degree-of-freedom system for various DR and for p=1.	19
2.9	Time-displacement traces of one-degree-of-freedom system for DR<1 and p=1.	21
2.10	Load-slip trace in cyclic-load test.	23
3.1	One-nail joint without spring for free-vibration test.	30
3.2	Two-nail joint with a spring for a free-vibration test.	31
3.3	Two connectors for fastening joints to wood frame in free-vibration test.	33
3.4	Testing arrangement applied in cyclic-load test.	38
3.5	Two-joint specimen for 18% Gap and 12% Gap Samples.	40
3.6	Flow chart for joint testing (i = sample type).	42
3.7	Loading diagram for static loading of samples.	46
4.1	Typical L-S traces for samples without gap (load levels are identified in Figure 3.7).	50
4.2	Typical L-S traces for samples with gap (load levels are identified in Figure 3.7).	51

List of Figures, continued

4.3	Typical digitized L-S trace of second loop at load level of 160 lb.	54
4.4	Relation between the MC and slip of tensile half-loops at tested load level for 12% No-Gap, Green, and 12% Cycling Samples.	59
4.5	Relation between the MC and slip of tensile half-loops at tested load level for Green, 18% Gap and 12% Gap Samples.	60
4.6	Relation between the load and slip of tensile half-loops for five MC samples investigated.	65
4.7	Relation between the load and slip of compression half-loops for five MC samples with smooth interface.	66
4.8	Relation between the load and slip of compression half-loops for five MC samples with rough interface.	67
4.9	Relation between the load and total energy absorbed per loop for five MC samples investigated.	68
4.10	Relation between the load and total energy capacity per loop for five MC samples investigated.	69
4.11	Relation between the load and damping ratio for five MC samples investigated.	71

LIST OF TABLES

Table		Page
3.1	Experiment types for free-vibration tests.	34
3.2	Sample types used in testing.	43
4.1	The number of specimen replications in test samples.	49
4.2	Significant level of F statistic for testing effects of moisture content, load level and inter-layer roughness.	56
4.3	Regression equations defining the effect of load level and moisture content on joint properties.	73
4.4	Significant level of F ratio for testing effect of interface roughness on slip of compression half-loops.	75
4.5	Comparison of damping ratio between joints with rough and smooth interface.	77

EFFECT OF DRYING ON DAMPING AND STIFFNESS OF NAILED JOINTS BETWEEN WOOD AND PLYWOOD

I. INTRODUCTION

Damping is the ability of a structure to dissipate energy during vibration [16]. Lazan [11] indicated three motivations in present-day study of damping. It has been used as a microstructural research tool for clarifying mechanisms that lead to inelastic behavior and energy dissipation on materials. A second motivation is its use as an inspection tool, such as to detect cracks in materials. A third motivation, and the one emphasized in this study, is the growing importance of damping as an engineering property in the analysis and design of machines and structures.

The importance of damping in structural analysis can be expressed in two ways: safety considerations and functional comfort [22]. Earthquakes and man-made explosions of high intensity could excite horizontal ground motions, which may cause the collapse of buildings [17]. Damping can greatly affect the stresses that cause the collapse; therefore, it is an important property in seismic structural analysis and design. Floors with low damping capacity can be objectionable to humans, even if vibrations caused by dynamic loads are small [3]. Recent design methods that will result in more economical, lighter, more flexible light-frame structures may make damping even more important than existing, often overdesigned, structures.

Nailed wood joints are commonly used in light frame construction, transferring forces in walls and floors from covering materials to studs or joints [3]. The contribution of internal material damping of wood in a structure built of components during vibration is of minor importance. Damping, and thus energy loss, is dominated by the frictional effects of joints [16].

Although frictional damping is inherent in most structures, there has been little attempt in the past to utilize its potential fully or to incorporate it as a design factor. There are two main reasons for this neglect: One, it depends on a variant quantity (i.e., the coefficient of friction), therefore it is not always easy to predict, especially if the effective forces cannot be completely specified; secondly, the frictional process may cause the surface conditions to change sufficiently over a period of time to render the original design assumptions invalid and the accompanying surface fretting may lead to shortened fatigue lives. Nevertheless, the increasing demand for additional structural damping has led to a renewed interest in frictional damping [5].

Stiffness is the resistance of materials and structures to deformation [2]. When a single nailed joint is laterally loaded, there is a relative displacement between the two wood members. This relationship between load and displacement is curvilinear, which traditional design neglects to recognize. Several recent investigations [2, 8, 12] were aimed at developing information for better understanding of the non-linearity of load-deflection relationships of nailed joints, thus leading to better design

specifications.

The main objective of this study was to develop the information on the effect on damping ratio and slip in nailed joints by changing moisture content in wood studs and the associated interlayer gap between wood and plywood. The second objective was to explore the possibility of using a free-vibration test in measuring damping ratio.

II. LITERATURE REVIEW

The stiffness and damping of a structure profoundly affect the safety and serviceability of the structure. The stiffness is important because it governs the structural resistance to static load. Under dynamic loads, damping, stiffness, and mass influence the dynamic properties, such as natural frequency and the rate of vibration decay [8].

This chapter defines the damping and stiffness of nailed joints. The discussion includes the sources of damping and two different expressions for damping. The discussion also contains pertinent papers dealing with stiffness and damping in nailed joints.

2.1 Damping

The damping phenomenon could be best illustrated by the free-vibration test of a beam. A weight, suspended from mid-span as shown in Figure 2.1, causes an initial displacement, X_o. A sudden load release, produced by cutting off the weight, initiates vibration that is illustrated by the deflection-time curve shown in Figure 2.2. The rate of diminishing deflection with time is related to damping.

2.1.1 Damping Sources in Wood Nailed Joints

Two basic damping sources are considered in this study: material damping of the wood, and slip damping, sometimes referred

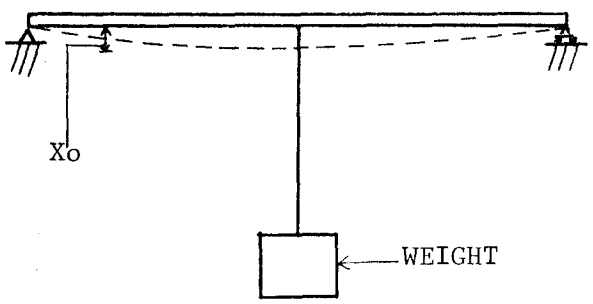

FIGURE 2.1 Free-vibration test of a beam.

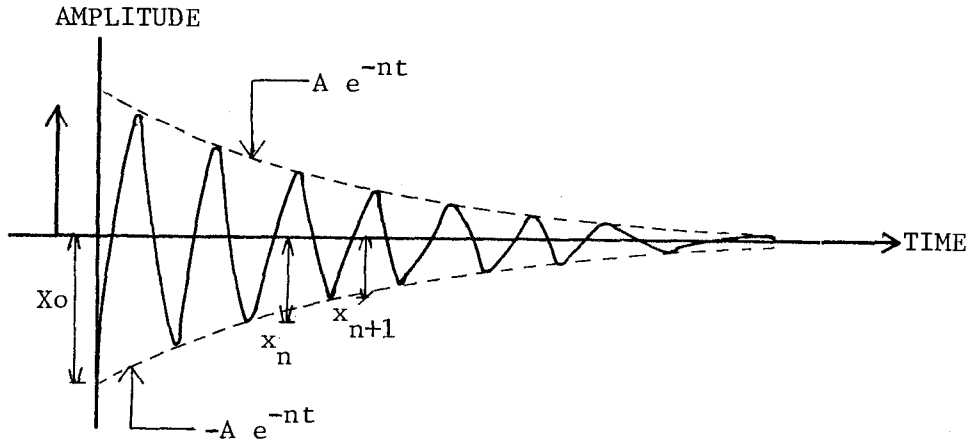

FIGURE 2.2 True displacement of beam against time in free-vibration test.

to as frictional damping, in the contact interface of nailed joints.

A typical nailed joint has a cross section as shown in Figure 2.3. When a cycling lateral load is applied to the joint, the nail is subjected to a shearing force which produces a bending moment in the nail and compression deformation in the wood [8]. If the load is sufficiently large, the nail is bent and the wood is deformed and a relative displacement between the sheathing and frame takes place.

Under increasing cyclic loadings, the deformed regions in the sheathing and lumber grow for each cycle, which is accompanied by energy dissipation in the wood and joint interlayer. The shape of deformation in the nailed joint is shown in Figure 2.4. The energy dissipated internally in the wood and plywood constitutes material damping, and the energy absorbed during the slip between the stud and sheathing plywood produces frictional damping.

2.1.1.1 Material Damping

The subject of material damping has been extensively reviewed by Lazan [11]. In the late sixties, Lazan reviewed and compiled the existing literature on damping of structural metals and concluded that the damping is stress-sensitive in the form:

$$D = J\sigma^n \tag{2.1}$$

where D is the specific damping or energy dissipated by damping for a unit volume at stress σ, J is the damping constant and n the

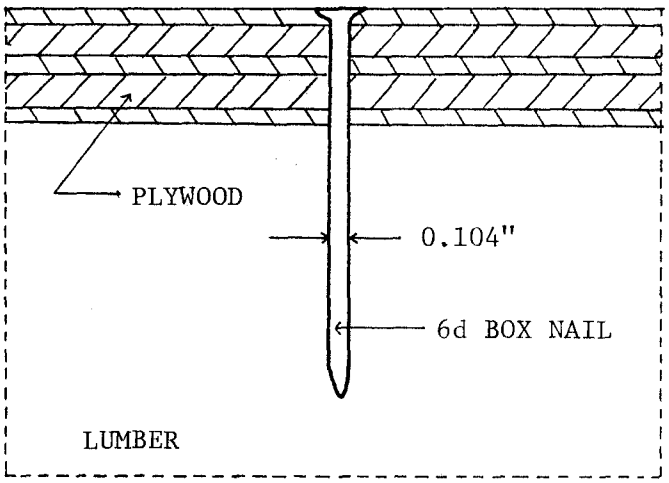

FIGURE 2.3 Cross section of a typical nailed joint.

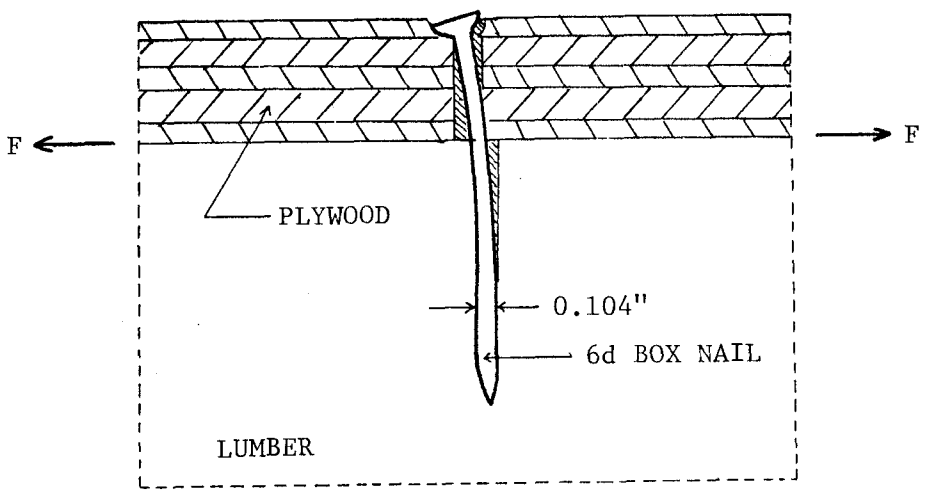

FIGURE 2.4 Hypothetical shape of deformation in the nailed joint.

damping exponent. The damping exponent lies between 2 and 3 in the low-intermediate stress region, but is much larger at higher stresses. For $\sigma < 0.8\ \sigma_f$, in which σ_f is the fatigue strength at 20×10^6 cycles, the damping is independent of stress history. For $\sigma > 0.8\ \sigma_f$, other variables, such as stress history, frequency and plastic deformation, start to influence damping.

Robertson and Yorgiadis [20] concluded from their experiments on metallic alloys and plastic materials that internal friction in materials, as represented by the damping, is independent of the frequency, proportional to the third power of the stress amplitude, and caused by the shear distortion in the material. These researchers also concluded that damping of most engineering materials is independent of frequency for very large frequencies.

During the past two decades internal material damping of wood has been investigated extensively, especially in low stress ranges. For instance, the damping ratio of maple wood was found to be 0.0037 [9]. Tests showed that damping ratio of Douglas-fir ranges from 0.0028 to 0.0092 in the moisture content interval between 0 to 20 percent and in the temperature interval from 0 to 200°F [7]. Additional information reported includes damping ratio of 0.0027 for cedar [13] and of 0.003 for spruce [10].

2.1.1.2 Frictional Damping at Contact Surfaces in Joints

For a structural member, if the stress is maintained within the working stress level, the material damping is normally small, and the total energy dissipation in a structure is usually dominated

by the interfacial frictional damping.

Connected elements in a joint are pressed together by the nail, which introduces interfacing pressure, N, that may be assumed to be uniformly distributed [22]. Subjecting this joint to a tangential force, F, as illustrated in Figure 2.5, produces a slip over a region along the length of the interface. Force F can be considered as the sum of the increments ΔFi acting along $\Delta Li(y)$.

$$F = \Sigma \Delta Fi \tag{2.2}$$

Because connected elements are very stiff compared to joint stiffness, the slipped region covers the whole interface and the slip is constant along the joint. The extent of $L_T(y)$ depends on N, the coefficient of friction and F. Unloading from F to zero is accomplished by reducing F by increments ΔF^i so that

$$F - \Sigma \Delta F^i = 0 \tag{2.3}$$

When ΔF^i is removed reverse slip occurs over $\Delta L^i(y)$ (Fig. 2.6) until Eq. (2.3) is satisfied. The resulting reverse slip equals

$$L_T(y) \simeq 2\, L^T(y) \tag{2.4}$$

because Yeh *et al.* [22] assumed that the effective coefficient of friction associated with $L^T(y)$ is about twice as large as $L_T(y)$. For steel, the factor 2 is not constant because of fretting on the interlayer. Thus, when Eq. (2.3) is satisfied, a state of self-equilibrating residual shear stress occurs in the interface. The response is not elastic and energy is dissipated. The energy

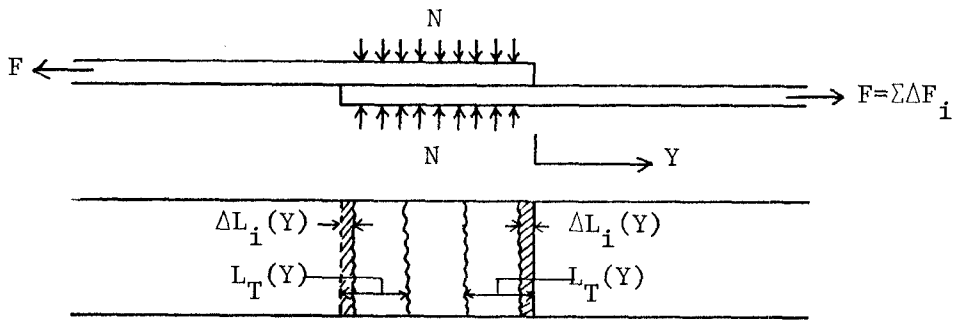

FIGURE 2.5 Loading situation in slip damping.

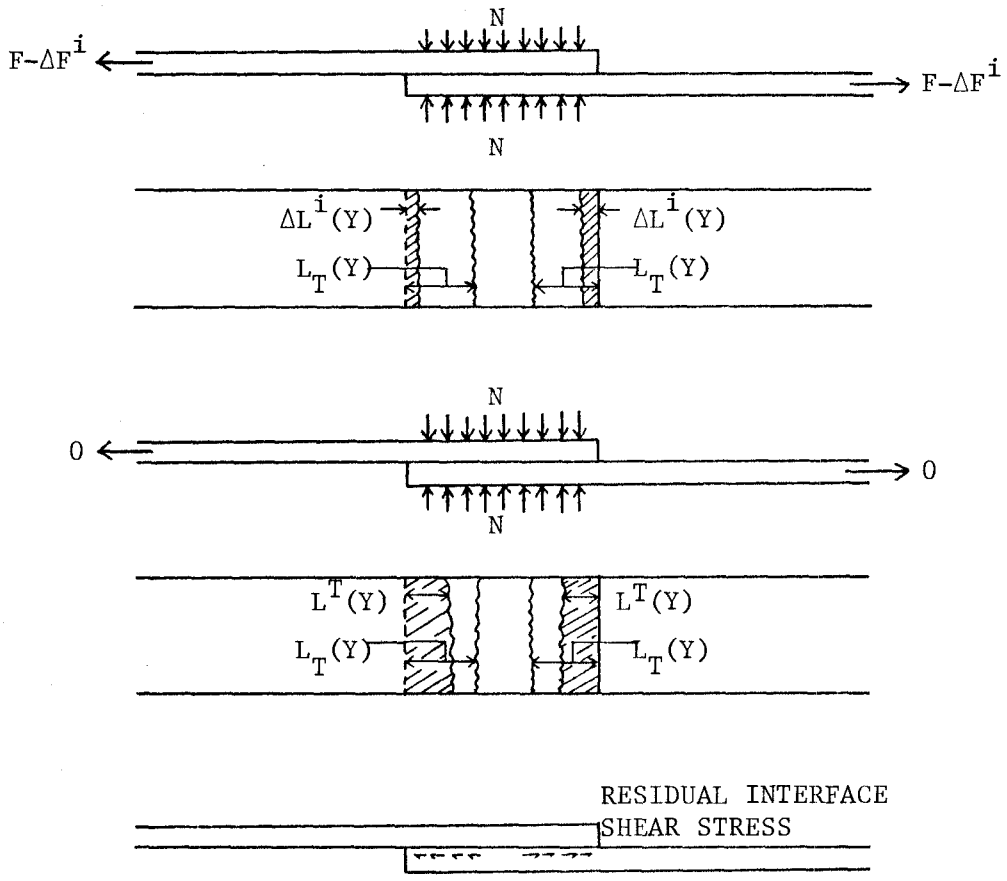

FIGURE 2.6 Unloading situation in slip damping.

dissipated in a cycle depends on F, the member thickness, coefficient of friction, N, the member breadth, and the modulus of elasticity of the connected materials. This mechanism does not produce linear damping, but Yeh et al. assumed it to be linear so they could solve the problem [22].

During the loading-unloading process, slip occurs and energy is dissipated. Several investigators [8, 22] agree that slip damping is much larger than material damping.

2.1.2 Theoretical Concepts of Damping Evaluation

Different investigators expressed damping in various ways, depending on the method of experimental measurement and analysis involved [8]. Damping ratio is usually used when analyzing structures for earthquake resistance [16]. To evaluate damping ratio, two major methods are commonly employed: dynamic free-vibration test and static cycling test.

2.1.2.1. Free-vibration Test

In a vibration system, shown in Figure 2.7, the differential equation governing the motion has a damping-associated force that is proportional to velocity [6]:

$$mx'' + CX' + kx = 0 \qquad (2.5)$$

in which m = mass

X = displacement

C = damping coefficient

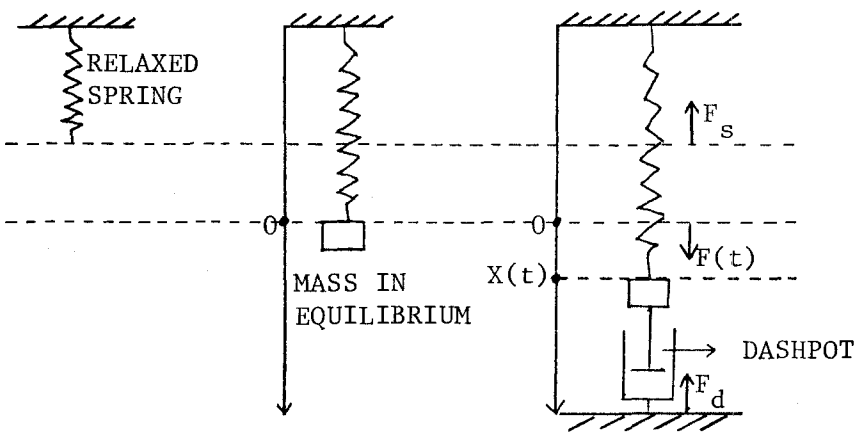

FIGURE 2.7 Single-degree-of-freedom system.

k = spring constant

and prime and double prime denote first and second derivatives with respect to time. The first term on the left side pertains to acceleration, the second to energy dissipated by damping, and the third to linear restoring force. Assuming $X = a \exp(rt)$ and substituting it into Eq. (2.5), gives

$$r^2 + (C/m)\, r + (k/m) = 0 \tag{2.6}$$

which has the roots:

$$r_{1,2} = -(C/2m) \pm \sqrt{(C^2/4m^2) - (k/m)} \quad (\text{if } C/2m > \sqrt{k/m}) \tag{2.7}$$

$$r_{1,2} = -(C/2m) \pm i \sqrt{(k/m) - (C^2/4m^2)} \quad (\text{if } C/2m < \sqrt{k/m}) \tag{2.8}$$

Eqs. (2.7) and (2.8) are equal when $C = 2\sqrt{km}$. This situation marks a critical limit of the viscous-friction factor C that places the vibrating system in one of two categories:

1. When $C > 2\sqrt{km}$, the viscous force governs the motion.
2. When $C < 2\sqrt{km}$, the inertia force prevails.

Thus, any vibrating system modeled by Eq. (2.5) has a parameter $Ccr = 2\sqrt{km}$ that, together with C, controls the magnitude of the force resisting vibration. Ccr is the system's critical value, which is of great importance in discussing its motion as the magnitude of C is varied. The ratio, DR, between these two parameters is essential to define this resisting force. It is defined as:

$$DR = (C/Ccr) = (C/2\sqrt{km}) \text{ or } C = 2\,DR\sqrt{km} \tag{2.9}$$

consequently Eqs. (2.5), (2.7), and (2.8) can be written as follows:

$$X'' + 2DRpX' + p^2 X = 0 \tag{2.10}$$

$$r = p\,(-DR \pm \sqrt{DR^2 - 1}) \quad \text{if } DR > 1 \tag{2.11}$$

$$r = p\,(-DR \pm i\sqrt{1-DR^2}) \quad \text{if } DR < 1 \tag{2.12}$$

in which $p = \sqrt{k/m}$. Substituting r in Eq. (2.11) into the original assumption $X = a\exp(rt)$ gives the solution for a system with large friction

$$X = \exp(-DR*pt)\,(a\exp(p\sqrt{DR^2-1}t) + b\exp(-p\sqrt{DR^2-1}t)) \tag{2.13}$$

If $a = (A+B)/2$ and $b = (A-B)/2$, then

$$X = \exp(-DR*pt)\,(A\cosh(p\sqrt{DR^2-1}t) + B\sinh(p\sqrt{DR^2-1}t)) \tag{2.14}$$

substituting the other two values of r in Eq. (2.12) into $X = a'\exp(rt)$ gives the solution for a system with small friction.

$$X = \exp(-DR*pt)\,(a'\exp(ip\sqrt{1-DR^2}t) + b'\exp(-ip\sqrt{1-DR^2}t)) \tag{2.15}$$

Using the identity $\exp(\pm iu) = \cos u \pm i \sin u$ in the above expression gives

$$X = \exp(-DR*pt)\,(A'\cos(p\sqrt{1-DR^2}t) + B'\sin(p\sqrt{1-DR^2}t)) \tag{2.16}$$

The motion of a system with viscous damping greater than the critical value Ccr is expressed by Eq. (2.14) which represents the condition of suppressed oscillation, because the hyperbolic functions of a real

variable are non-periodic. The motion of a system with viscous damping smaller than Ccr is expressed by Eq. (2.16) that describes a damped periodic motion with a natural frequency of $p\sqrt{1-DR^2}$ and damping factor of exp(-DR*pt). For DR = 1, and r = -p, Eq. (2.16) becomes

$$X = a''\exp(-pt) + b''t\exp(-pt) \tag{2.17}$$

which shows that the motion with critical damping is not periodic.

Next, the general starting condition is evaluated that is based on $X=X_o$ and $X'=V_o$ when t=0. This gives

$$X = \exp(-DR*pt)\ (X_o\cosh(p\sqrt{DR^2-1}t) + (V_o + DRpX_o)/(p\sqrt{DR^2-1})\ (\sinh(p\sqrt{DR^2-1}t))) \quad \text{for DR} > 1 \tag{2.18}$$

$$X = \exp(-DR*pt)\ (X_o\cos(p\sqrt{1-DR^2}t) + (V_o + DRpX_o)/(p\sqrt{1-DR^2})\ (\sin(p\sqrt{1-DR^2}t))) \quad \text{for DR} < 1 \tag{2.19}$$

and $$X = \exp(-DR*pt)\ (X_o + ((V_o + DRpX_o)/p)pt) \quad \text{for DR} = 1 \tag{2.20}$$

Assuming that $V_o=0$, $X_o=1$, and that p is 1 radian per sec. lead into following discussion. Figure 2.8 illustrates a time plot of the displacement of the system with single-degree-of-freedom for several values of the damping ratio, DR, and the attenuation curve of exp(-pt). A system, with DR=0, has zero friction and reaches the static-equilibrium position of X=0 in $\pi/2$ sec. which is the minimum time required. For DR=1, the system is critically damped and C has a critical value of $2\sqrt{km}$, that is the system

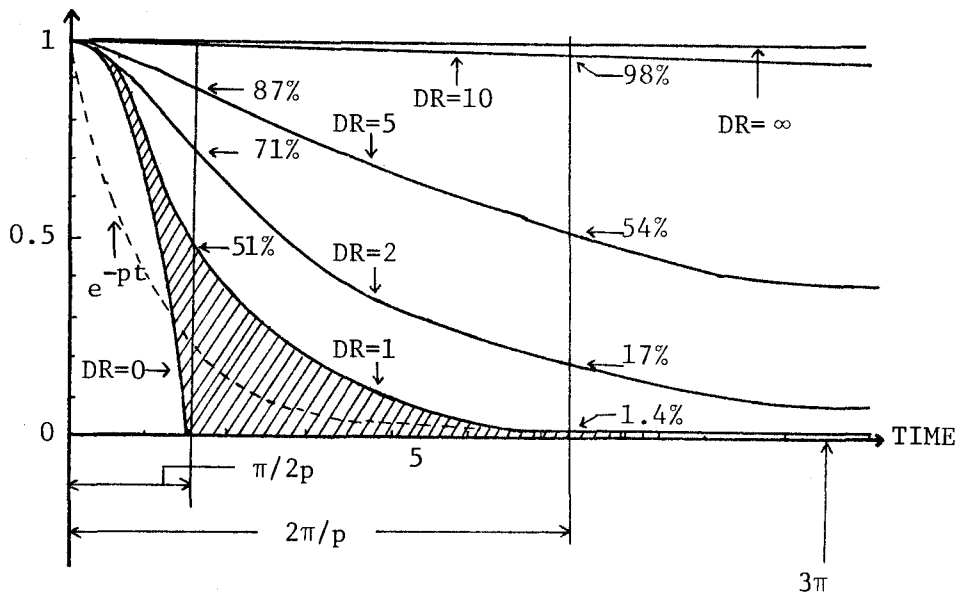

FIGURE 2.8 Time-displacement traces of one-degree-of-freedom system for various DR and for p=1.

comes to rest at the static-equilibrium position. This case is sometimes referred to as that of the minimum amount of viscous damping for aperiodic motion. For large values of damping with DR > 1, the motion is non-oscillatory. Moreover, the time necessary for the system to reach the static-equilibrium position becomes infinite, as the system comes to rest in a position of a static deflection often called a permanent set.

Structural systems in the real world have DR's between zero and unity [6]. Figure 2.9, depicting a family of free-vibration curves for ranges of DR between zero and unity, shows that increasing the viscous friction will have two effects: the displacement attenuation and the lengthening of the natural period.

Damping ratio, DR, from free-vibration tests is evaluated first by combining the two trigonometric terms of Eq. (2.19):

$$X = \exp(-DR*pt)\sqrt{X_o^2 + ((V_o + DRpX_o)/(p\sqrt{1-DR^2}))^2}\cos(p\sqrt{1-DR^2}t-\phi)$$

$$\tan\phi = (V_o + DR*pX_o)/(X_o p\sqrt{1-DR^2}) \qquad (2.21)$$

in which ϕ = phase angle. The successive positive and negative maximum values of X occur at time interval corresponding to one full cycle of the trigonometric term, $2\pi/(p\sqrt{1-DR^2})$. Therefore, successive positive or negative displacement values that are located one cycle apart have a ratio

$$X(n+1)/X(n) = \exp(-DR*pT) = \exp(-2\pi*DR/\sqrt{1-DR^2}) \qquad (2.22)$$

in which T is period or time elapsed during one cycle. It should not be based on the time interval between the start and the first

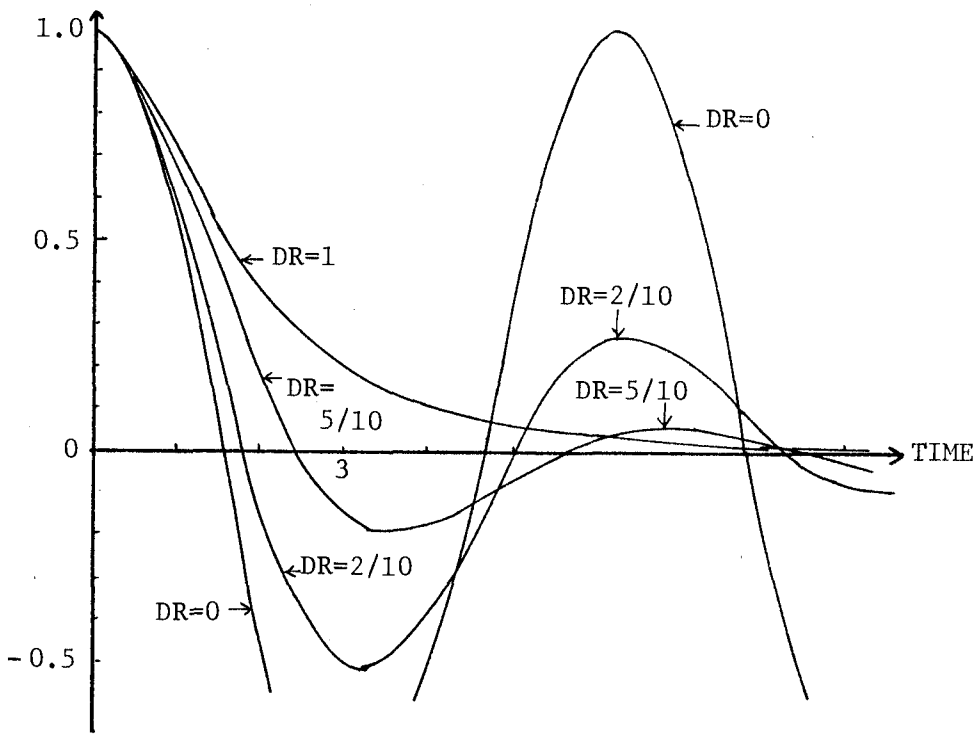

FIGURE 2.9 Time-displacement traces of one-degree-of-freedom system for DR < 1 and p=1.

crossing of the time axis, because this time equals $(\pi/2 + \phi)/(p\sqrt{1-DR^2})$ sec. and not T/4.

For small values of DR

$$X(n+1)/X(n) \simeq \exp(-2\pi DR) \tag{2.23}$$

or

$$DR \simeq (1/2\pi) \quad \ell n \quad (X(n)/X(n+1) \tag{2.24}$$

The quantity $\ell n\ (X(n)/X(n+1)) = 2\pi DR/\sqrt{1-DR^2}$ is known as logarithmic decrement and is often used in measuring structural damping.

2.1.2.2 Cyclic-load Test

For wood-based joints the load-deflection traces from static cyclic-load tests are nonlinear, which complicates the exact analysis of joint damping [14]. At loads recommended for structural analysis and design, the curves are similar to that shown in Figure 2.10. Such experimental curves are often used to evaluate damping that is equivalent to viscous damping discussed above [6]. The total dissipated work per cycle, Δw, and associated energy absorption, EA, is represented by the area of the hysteretic loop ABDEA (Fig. 2.10). Assuming that all of the curve's nonlinearity is due to damping, so that the restoring force can be represented by the line EOB, the total work capacity, W, and associated energy capacity per cycle, EC, equals the area OBCOEFO. The ratio of $\Delta W/W$ or EA/EC, defines the damping. For wood-joint specimens, this ratio is not constant, but it changes with the load and deflection.

For DR < 1, EA is equal to the work done by the viscous damping

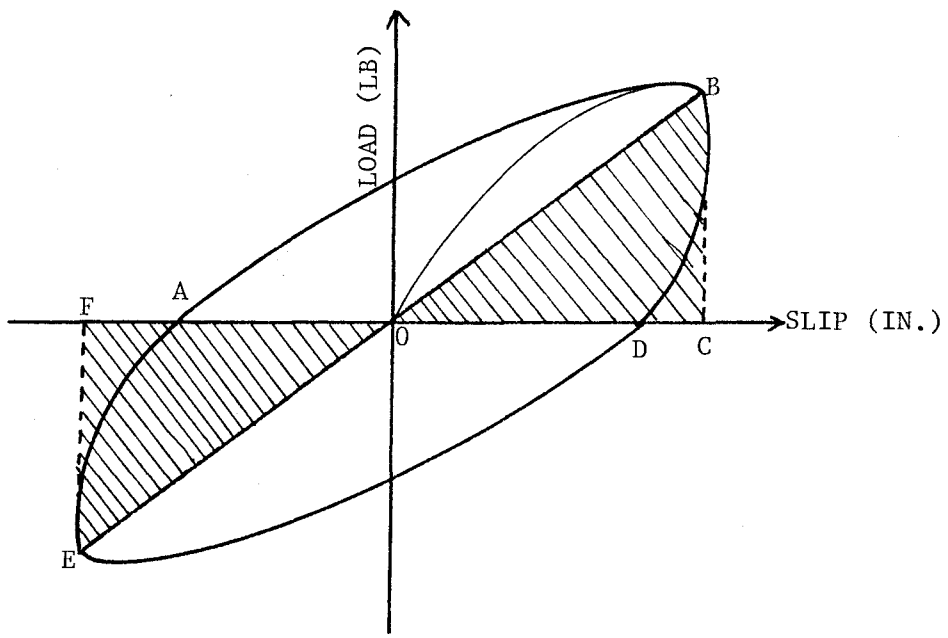

FIGURE 2.10 Load-slip trace in cyclic-load test.

forces, CX', either per half or full cycle of vibration. Thus, by knowing the kinetic energy of the system at times $t=t_o$ and $t=t_o+T/2$, where T is the period of vibration and equal to $2\pi/(p\sqrt{1-DR^2})$, the difference between these two energies equals EA/2

$$EA = 2*[K.E.(t=t_o) - K.E.(t=t_o+T/2)] \tag{2.25}$$

The kinetic energy is defined by

$$K.E. = 1/2\ m(X')^2 \tag{2.26}$$

Incorporating the initial condition $X_o=0$ and differentiating Eq. (2.19) gives

$$X' = \exp(-DRpt)\ X_o' \cos(p\sqrt{1-DR^2}t) - (DR/\sqrt{1-DR^2})\ \exp(-DRpt)\ \sin(p\sqrt{1-DR^2}t) \tag{2.27}$$

At $t=t_o=0$ and $t=T/2$, the velocity equals $X'(t=0)=X_o'$ and $X(t=T/2)=(-\exp(-DR*pT/2))X_o'$, respectively. Thus, EA is

$$EA = m(X_o')^2(1-\exp(-DR*pT)) \tag{2.28}$$

The energy capacity of the system is equal to the strain energy (S.E.) of the system at maximum displacement. Because of damping this displacement does not occur exactly at t=T/4, so the energy capacity, EC, also includes K.E.:

$$EC = 2*[K.E.(t=T/4) + S.E.(t=T/4)] \tag{2.29}$$

$$S.E. = 1/2\ kX^2 \tag{2.30}$$

in which X is determined from Eq. (2.19):

$$X(t=T/4) = (\exp(-DRpT/4)X_o')/(p\sqrt{1-DR^2}) \tag{2.31}$$

from which

$$X'(t=T/4) = -((DR*p\ \exp(-DR*pT/4)X_o')/(p\sqrt{1-DR^2})) \tag{2.32}$$

Using Eqs. (2.29), (2.31), (2.32), in conjunction with the relationship $p^2 = k/m$, gives

$$EC = 1/2\ m(X_o')^2\ \exp(-DR*pT/2)\ ((1+DR^2)/(1-DR^2)) \tag{2.33}$$

Thus, energy ratio equals

$$EA/EC = ((1-DR^2)/(1+DR^2))((\exp(DRpT/2))-(\exp(-DRpT/2))) \tag{2.34}$$

Substituting the known relationships, $T = 2\pi/p\sqrt{1-DR^2}$ and $\exp(t)-\exp(-t) = 2\sinh(t)$, gives

$$EA/EC = ((1-DR^2)/(1+DR^2))\ 2\ \sinh(DR*\pi/\sqrt{1-DR^2}) \tag{2.35}$$

If DR is small, further simplification can be made:

$$2\ \sinh(DR*\pi/\sqrt{1-DR^2}) \simeq 2\pi DR \tag{2.36}$$

and

$$EA/EC \simeq 2\pi DR \tag{2.37}$$

2.2 Stiffness

When a nailed joint is laterally loaded, a relative displacement takes place between the connected members due to deformation of wood fibers and nail bending. This displacement is referred to as slip [12]. The stiffness of joints is measured by the slip

modulus that is defined as the slope of the lateral load vs. slip. The load-slip trace is nonlinear except for a very small initial part of the trace.

The stiffness of wood structures is important because it governs the deflection that is an important design parameter [8]. There are four variables influencing the load-slip relationship: wood characteristics, nails, loads and joint configuration. Antonides [2] presented a comprehensive review of these influencing variables. The values of slip corresponding to specified loads were acquired to represent the stiffness of the nailed joints in this study.

2.3 Review of Pertinent Literature

Atherton [4] tested single-nail joints under loads consisting of four fully reversed cycles in the positive and negative loading domains at five load magnitudes. He evaluated effects of specific gravity, foundation modulus of wood and plywood, and plywood thickness on slip modulus and energy absorption. He found that load magnitude had the greatest effect of all variables and that the effect of load-cycling, specific gravity, positive-negative loading, plywood thickness and foundation modulus was also present ranging from negligible to moderate. However, Atherton also found that these effects were not consistent.

Kaneta [8] made both theoretical and experimental studies of joint damping and stiffness. He indicated that the main sources of damping were the friction between framing and sheathing

materials and the plastic yielding of the wood in the neighborhood of the nail. He concluded that the load-deflection characteristics of composite framed panels can be determined from experimental data available with reasonable accuracy whenever their loading conditions are prescribed.

Young and Medearis [24] tested to failure eight shear walls of size 8- by 8 ft and of 2- by 4 in. framing sheathed with plywood. The loading consisted of fully reversed positive-negative cycling. They determined overall damping ratio of the panels and evaluated the importance for damping in earthquake design.

Polensek [17] dynamically tested eleven roof diaphragms and constructed a logarithmic regression equation between the damping ratio and diaphragm stiffness. He stated that his results were useful in the analysis of wood buildings subjected to horizontal vibrations caused by earthquakes and explosions. Polensek [16] also investigated the damping of nailed wood-joist floors by vertical- and horizontal-free-vibration tests. The average damping ratio for the tested floors ranged between 0.04 and 0.06 for vertical vibration and between 0.007 and 0.11 for horizontal vibration.

Yeh [23] studies slip and damping in nailed and glued I-beams made of lumber. He employed pre-bored nail holes in coverings to eliminate nail-bearing effect on joint stiffness. Damping at the interface of plywood and lumber was controlled by a spring under the nail heads that exerted pressure against the plywood. Specimens were subjected to static cycling loads up to 100 cycles. He developed a theoretical model that uses the results from tests of one-nail

joint specimen to predict overall damping ratio of the T-beam made with lumber and plywood. However, the model predictions correlated poorly with experimental results.

Wilkinson [21] vibrated single-nail lap joints loaded longitudinally and measured acceleration. He stated that damping was not important in his experiment, and that stiffness of wood joints increases appreciably when subjected to vibrational loading as compared to static loading. This conclusion is of no surprise, because his study was mostly aimed at evaluating the linear part of the load-slip curve.

III. EXPERIMENTAL PROCEDURE

3.1 Procedure Selection

In the past, researchers have measured damping ratio by testing full-scale wood panels or single-nail joints under cyclic loading. For instance, Polensek conducted free-vibration tests on wood-joist floors [16, 19] and roof diaphragms [17], and Wilkinson [21] applied forced vibration to nailed and bolted wood joints. However, no researcher employed free-vibration tests on single-nail joints. Therefore, preliminary tests were conducted on single-nail joints to explore the feasibility of using a simple free-vibration test to determine the damping ratio.

3.1.1 Preliminary Testing

Nailed joints were made of Douglas-fir studs and of either 19/32-in., 5-ply sheathing plywood or 1/2-in. gypsum wallboard. The first-trial specimens consisted of one-nail joints as shown in Figure 3.1 Two 900-gram steel weights were fastened to the sheathing material in an attempt to increase the inertia forces needed to induce the vibration. Because no free vibration could be produced by this arrangement, a tension/compression spring was fastened to stud and sheathing (Fig. 3.2) to increase the potential energy of the joint under initial slip used to start the free vibration. The stiffness modulus of the spring was 1300 lb/in.

All tests were conducted in the Standard Room, a conditioning room maintained at a constant temperature of 70°F and relative

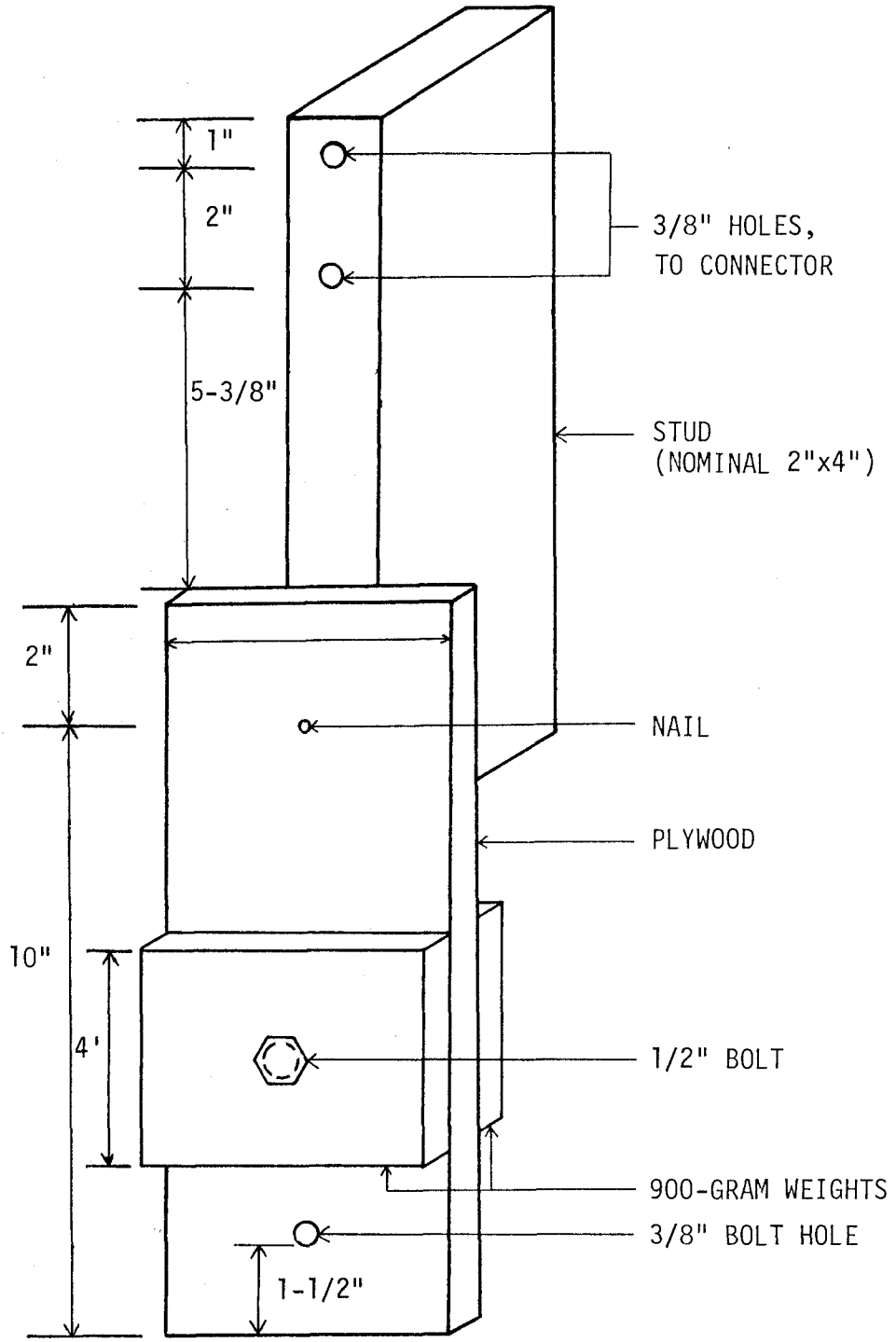

FIGURE 3.1 One-nail joint without spring for free-vibration test.

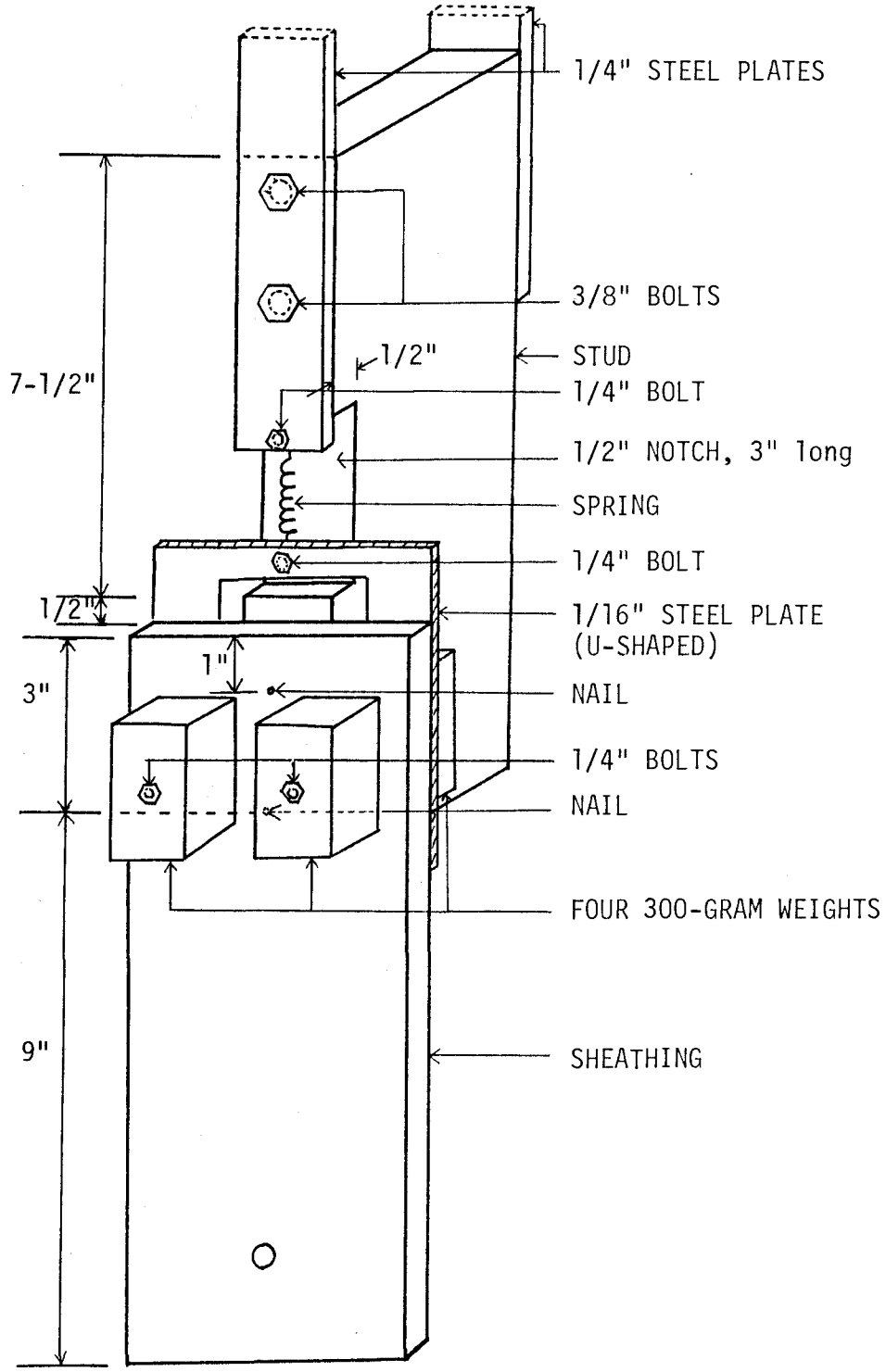

FIGURE 3.2 Two-nail joint with a spring for a free-vibration test.

humidity of 65 percent. This condition produces in wood a 12 percent moisture content (MC). The stud portion of the joint was fastened to a rigid, self-standing wood frame (Fig. 3.3). A linear variable differential transducer (LVDT) attached to the stud and sheathing was used to measure the joint slip or relative displacement of the stud and sheathing. The signal from LVDT was monitored by an oscillograph that recorded a continuous slip vs. time trace of vibrating specimens.

Initial slip was introduced by the weight of either 40, 80, 120, or 160 lb, suspended from the sheathing material by the piano wire. Vibration was initiated by cutting the suspended weight off the specimen. Seven types of experiments, Experiments I through VII (Table 3.1), were conducted to explore the feasibility of evaluating the damping ratio.

The results of Experiment I were inconsistent; some of the time-deflection traces showed vibration about the static equilibrium position, others did not. Therefore, subsequent experiments were modified in an attempt to achieve more consistent dynamic response.

The first modification (Experiment I, II and III) consisted of attaching a mass to the center of the plywood section (Fig. 3.1 and Table 3.1), but the added masses did not always produce the vibration. The second modification (Experiment II and III) consisted of using smaller nails in addition to the attached mass. Again, some specimens displayed dynamic response while others behaved statically. This inconsistency was probably due to bending and torque about the nail, which could have rotated the plywood section of some specimens

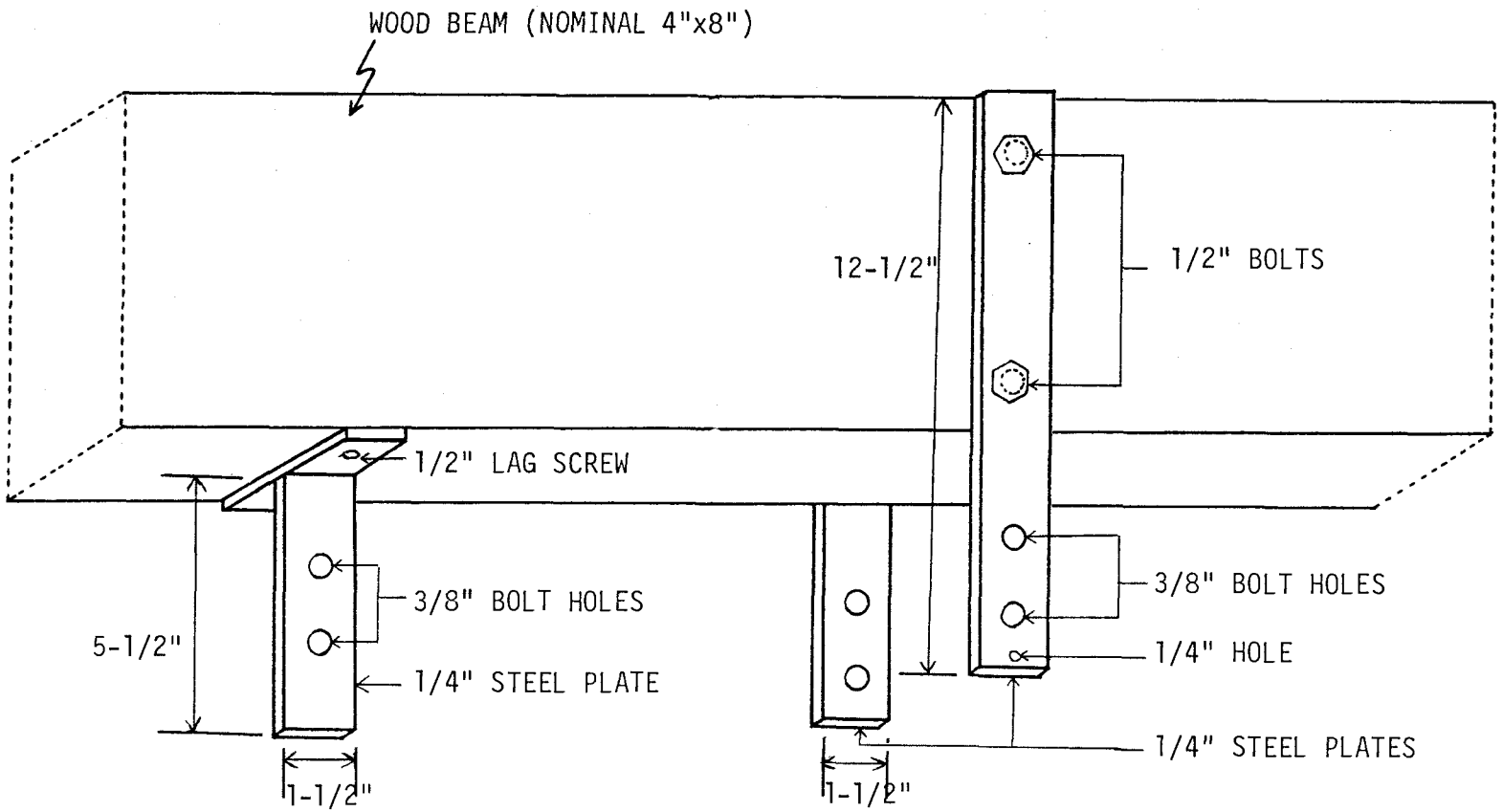

(a) For specimen shown in Figure 3.1 (b) For specimen shown in Figure 3.2

FIGURE 3.3 Two connectors for fastening joints to wood frame in free-vibration test.

Table 3.1 Experiment types for free vibration-tests.

Experiment type	Joint type*	Sheathing material	Nails		Additional mass	Spring	Initial weight(lb)
			Type	No.			
I	A	plywood	7d	1	No or Yes	No	40,80,120,160
II	A	plywood	4d	1	No or Yes	No	40,80
III	A	plywood	3d	1	No or Yes	No	40,80
IV	A	plywood	4d	2	No	No	80,120,160
V	A	plywood	3d	2	No	No	80,120,160
VI	B	plywood	6d	2	Yes	Yes	40,80,120,160
VII	B	gypsum board	6d	2	Yes	Yes	40,60,80

*A: identified in Figure 3.1,
B: identified in Figure 3.2.

during testing. Experiments IV and V were designed to verify this hypothesis. Two nails, spaced 2 in. along the stud, were used on each joint to prevent bending and torque. Now, all the specimens behaved statically. Thus, the vibration of joints in Experiments I through III were not caused by the shear slip but by bending and torque. Therefore, a spring was added to increase the recoverable potential energy of the joint under initial load (Experiment VI). Again, the results showed no vibration, possibly because the spring was not stiff enough for the joint used. Therefore, gypsum wallboard was used instead of plywood to reduce the joint stiffness (Experiment VII). In this arrangement, the specimens finally responded dynamically to the initial slip under 40-lb load.

Experiment VII consisted of nine replications. The resulting damping ratio from the free-vibration time-slip traces had a mean of 0.0561 and standard deviation of 0.00823.

To compare the free-vibration damping ratio to those of cyclic-load tests, 18 single-nail joints of stud and gypsum wallboard sections were tested under static cyclic load. The mean of these damping ratios was 0.2286 with a standard deviation of 0.00492. The difference between the two means indicated additional potential problems associated with the free-vibration test, which were not detected by the preliminary investigation. Therefore, additional experimentation was discontinued, because further improvements would complicate already difficult-to-construct specimen assembly and testing.

3.1.2 Procedure Evaluation

Free-vibration tests can be meaningful only when the specimen contains enough potential energy to induce vibration. Vibration can be induced by a proper combination of mass, joint stiffness and added spring. However, the resulting procedure is cumbersome and not fully reliable. Therefore, the already established procedure with static cyclic loading, used by other investigators, was chosen for this study.

3.2 Materials and Methods

This section covers the description of materials, specimens, testing arragnements and variables employed in the cyclic-load tests of nail joints. When physically possible, the same plywood and stud sections were used to construct samples of matched specimens.

3.2.1 Material Selection and Specimen Construction

Studs. Twenty-five Douglas-fir studs of nominal 2- by 4-in. size were selected from an unused portion of the material that remained from a recent research project. The studs had been kiln-dried and stored in a covered shed at an equilibrium MC of about 12 percent. A section of 12-in. length was cut from each stud, which gave a sample of twenty-five replications. Sections were withtout any obvious defects, such as knots, wane and slope of grain. After cutting, each section was weighted, coded and measured for MC with a resistance-type electric moisture meter. To

provide the means of connecting the wood sections to the testing apparatus, two 3/8-in. bolt-holes, 1 and 9/16 in. apart, were drilled parallel to the wide face through the center of the narrow face, 5/8 in. away from the end of each section (Fig. 3.4). Afterwards, the stud sections were equalized in the Standard Room for about one year.

Plywood. Three 4- by 8-ft sheets of 19/32-in., 5-ply Douglas-fir plywood of sheathing grade were purchased from a local lumber yard. Each sheet was cut into 4-in. by 8-ft strips with the face grain oriented parallel to 8-ft side. Each strip was then cut into eight 12-in. sections. The pieces that contained defects, such as knots and gaps between laminations, were discarded. A center line was drawn on each piece, parallel to the 12-in. axis, and two 3/8-in. holes, 1 and 9/16 in. apart, were drilled through the center line 5/8 in. away from one of the 4-in. edges (Fig. 3.4). This edge was designated as the bottom edge, because it was on the bottom during testing. The two holes were provided for connecting the specimen to the testing machine. After manufacturing, the sections were conditioned in the Standard Room for about one year.

Nails. Six penny, galvanized, smooth, box nails were used for all specimens. They were of the same manufacture and taken from the same keg. The nails were 2 in. long with an average shank diameter of 0.104 in. and head diameter of 0.28 in.

Assembly. To assure a precise nail placing, center lines were drawn parallel to the 12-in. axis on the narrow face of each stud

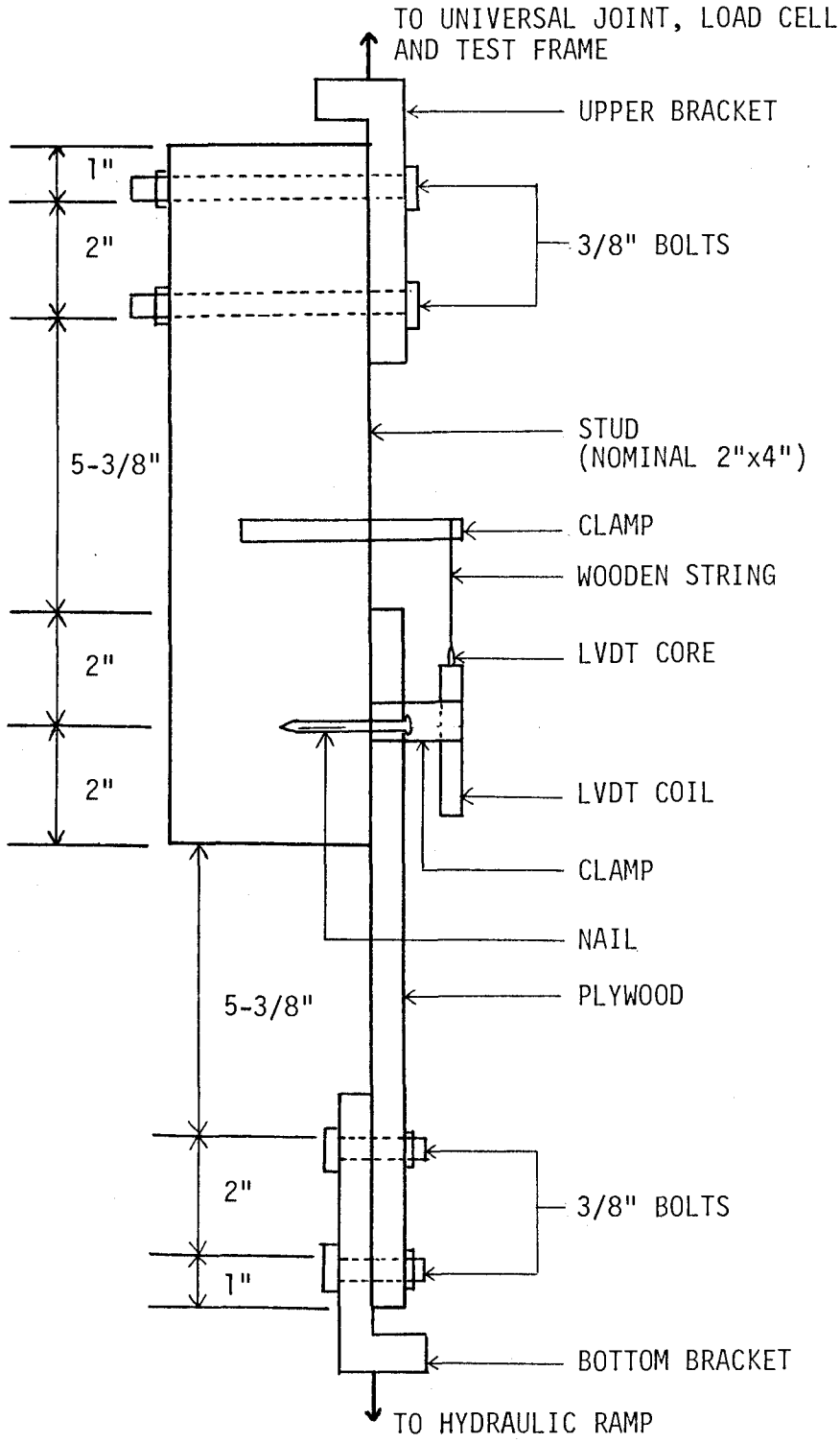

FIGURE 3.4 Testing arrangement applied in cyclic load test.

section. Specimens were assembled in steps. First, the plywood section was positioned to the narrow face of the stud section, so that the center lines of both pieces coincided and the length of the contact surface or interface became 4 in. Then the nail was hammered into both sections exactly at the geometric center of the interface, 2 in. away from the edge of stud and plywood. Figure 3.4 illustrates an assembled specimen ready for testing. After each test, the specimens were disasembled and 1-in. strips were cut off from the stud and plywood section near the previous nail sites. For the next specimen constructed from this plywood and stud section, the new nail sites were moved 1 in. along the center lines of the sections. The interlayer length again was 4 in.

Two-joint specimens were also used in this study, one for testing joints with gaps dried from green to 18 percent MC, and the other for testing joints with gaps dried from green to 12 percent MC. The two-joint specimens had plywood sections nailed to both narrow faces of the stud section in the same operation (Fig. 3.5). The handling and testing of the 18 percent joint was conducted very carefully to avoid damaging the 12 percent joints.

The two-joint specimens were constructed as follows. Twenty-five 12-in. stud sections of nominal size 2- by 4 in. and fifty 4- by 12-in. plywood sections were stored in the Standard Room until they reached 12 percent MC. Each stud had two narrow faces of 1.5-in. width, one was smoother than the other due to machining. Both stud sides were used in testing. Thus, for one test, twenty-five plywood sections were nailed to the smooth side of twenty-five stud

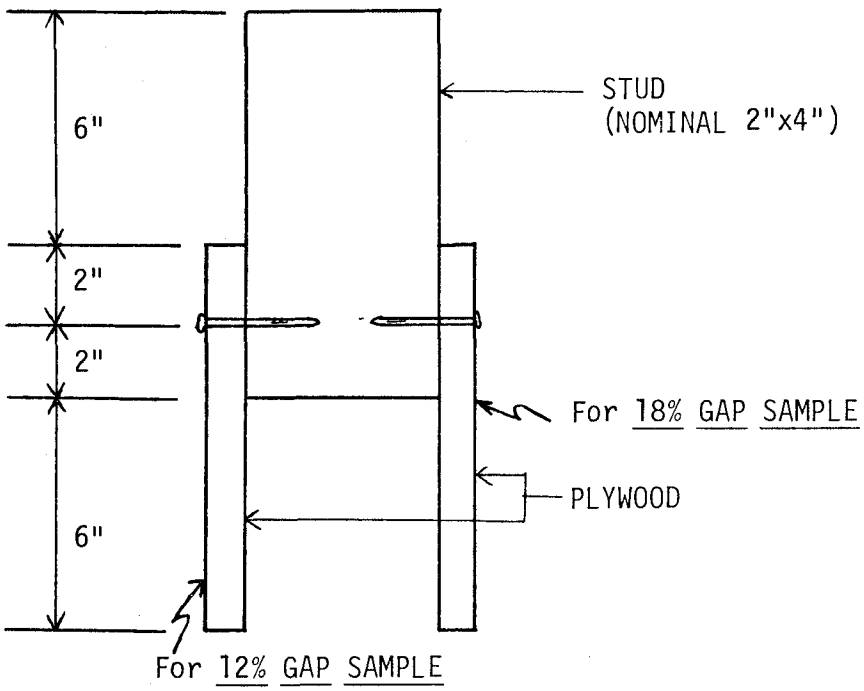

FIGURE 3.5 Two-joint specimen for 18% Gap and 12% Gap Samples.

sections, and for another test, twenty-five plywood sections were nailed to the rough side of the stud sections.

3.2.2 Experimental Design

The main objective of this experiment was to determine the effect of changing MC of stud section on the damping ratio and slip.

Figure 3.6 shows a flow chart of the experimental method and Table 3.2 illustrates the sample types used in testing. A total of five samples was tested, each sample with studs of a different MC. The first (in the flow chart, i=1) was constructed dry and tested dry (12% No-Gap Sample), the second (i=2) was constructed green and tested green (Green Sample), the third (i=3) was constructed green and tested at 18 percent MC (18% Gap Sample), the fourth (i=4) was constructed green and tested at 12 percent MC (12% Gap Sample), and the fifth (i=5) was constructed dry from studs that had been conditioned by a moisture cycle of dry-green-dry and tested dry (12% Cycling Sample).

In 12% No-Gap Sample, the smooth-interface joints were tested first, then the plywood sections were removed, and twenty-five new plywood sections were nailed to the rough-side of the stud. Thus, the total test number for this sample became fifty. After the sample was tested and disassembled, the recovered stud sections were placed in a pressure tank full of water for four days to reach the fiber saturation point. The pressure in the tank was set to a relatively low value of 20 psi to prevent material damage. Then the stud sections were used to construct the specimens for Green

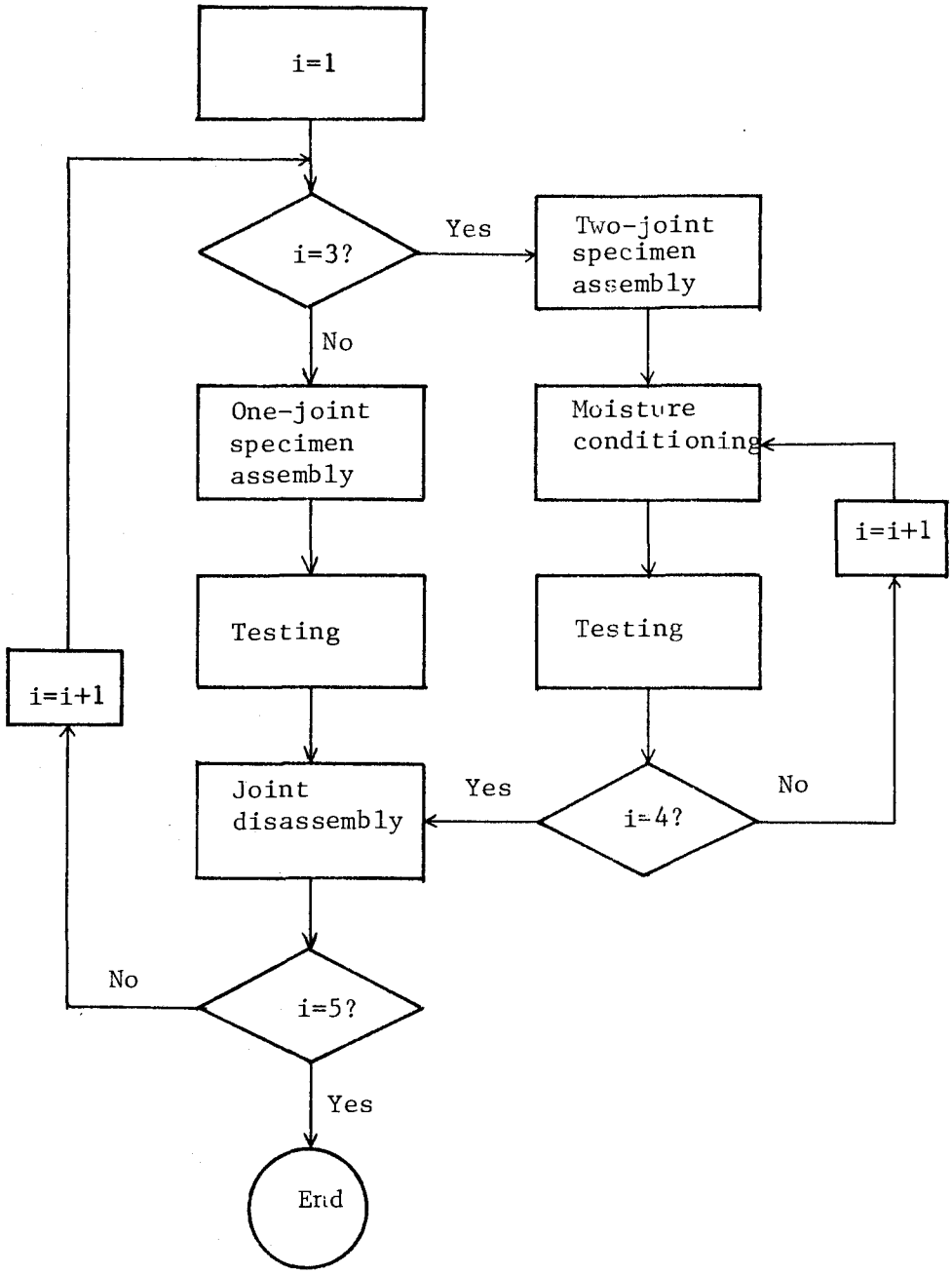

FIGURE 3.6 Flow chart for joint testing (i=sample type).

Table 3.2: Sample types used in testing.

Sample			Stud moisture content(%)		
Name	type	Size	At assembly	At testing	Gap
12% No-Gap Sample	1	50	12	12	No
Green Sample	2	50	28	28	No
18% Gap Sample	3	25	28	18	Yes
12% Gap Sample	4	25	28	12	Yes
12% Cycling Sample	5	50	12	12	No

Sample. After testing the Green Sample, two-joint specimens (Fig. 3.5) were assembled with stud sections still in green condition. The resulting twenty-five specimens with 50 joints were placed into the Standard Room to dry. To accelerate the drying rate, a mild fan was used to circulate the air around the specimens. When MC in studs reached about 18 percent, thirteen smooth-interface and twelve rough-interface joints on one side of each two-joint specimen were selected at random to provide specimens for the 18% Gap Sample. After testing this sample, the specimens, now each having only one untested joint, were placed again into the Standard Room for further drying. These specimens with twelve smooth- and thirteen rough-interface joints formed 12% Gap Sample and were tested when MC in stud sections reached 12 percent. Term "gap" in the sample name underlines the fact that a gap, large enough to be visible, developed between the stud and plywood sections due to wood shrinkage during drying.

The target MC in stud sections of 12% Cycling Sample was the same as that of 12% No-Gap Sample. The difference between these samples is the preconditioning of the stud piece before joint assembly in 12% Cycling Sample. The specimens in this sample displayed no gap between the stud and plywood sections.

3.2.3 Testing Arrangement

The assembled joints were mounted to the testing machine by brackets attached to the test frame that minimized the bending on the joint (Fig. 3.4). The bending effect was small, because the

applied force acted through the line that was parallel and very close to the joint interface. The slip was monitored by an LVDT and the load cell provided the signal that measured the applied load.

The mounting procedure began by first placing the two top bolts through the holes of the stud section and the upper mounting bracket (Fig. 3.4). The LVDT body (coils) was positioned parellel to the stud length and clamped to the plywood section. Then the LVDT magnet core, attached to the wooden stick, was inserted into the coils. The wooden stick was clamped to the stud section without touching the plywood section. After inserting the core into the coils, the bottom bolts were placed through the plywood section and the bottom bracket. Finally, the adjustment screw, which was on top of the wooden stick, was turned until reaching the zero-voltage output of the LVDT.

The load cell was placed between the upper universal joint and test frame (Fig. 3.4). The signals from both the load cell and LVDT were continuously recorded by an X-Y recorder. The slip was measured to 0.0001-in. accuracy and the load to 0.1-lb accuracy.

3.2.4 Testing Procedure

The testing was performed in the Standard Room, which minimized the disruption in the conditioning of the specimen. All the samples were subjected to cyclic loading at five load levels (Fig. 3.7). Initial loading direction was the one that pulled the joint components away from each other; when applied in this direction, the loading will be referred to as a tensile load. Then load was

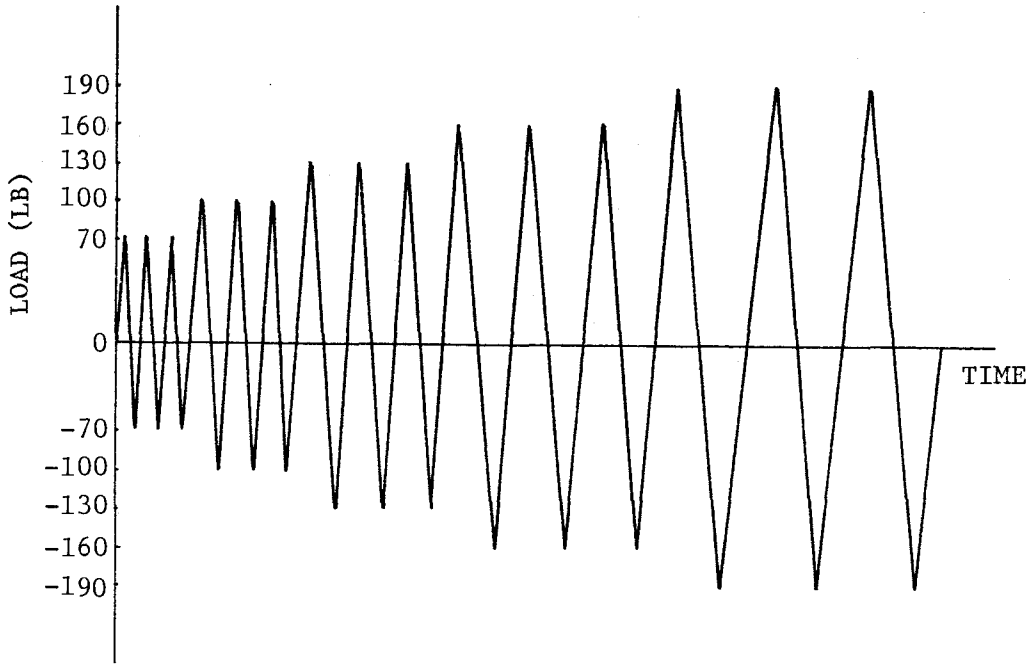

FIGURE 3.7 Loading diagram for static loading of samples.

changed to opposite direction to complete the cycle; the loading in this direction will be referred to as a compression load. At each load, there were three fully reversed cycles (Fig. 3.7). The loading rate was 1.5 in./min. which is about 10 times faster than that recommended by the ASTM [1]. The faster loading rate was chosen to speed up the testing and to reflect the current trends in the testing community toward faster loaded rate in testing.

IV. RESULTS AND DISCUSSION

This chapter covers the data analysis techniques, presents the reduced data, and discusses the most important results that were derived from the experiments described in Chapter III.

4.1 Experimental Data

The original work plan called for testing of two hundred specimens. However, because of difficulties with nail driving and scale selection, 188 usable load-slip (L-S) traces were obtained. Total number of replications in each sample is summarized in Table 4.1.

Figures 4.1 and 4.2 illustrate typical L-S traces obtained in testing. These traces, visualized as a set of hysteresis loops, are often nonsymmetrical; that is, they have their axes of zero slip moved away from those of the initial half-loops. This is probably due to the loading sequence used in testing; the initial half-loop loading could have bent the nail and the succeeding loading in the opposite direction could not straighten the nail which retained the initial bending mode throughout the testing.

The half-loops, shown in Figures 4.1 and 4.2 above the slip axis and associated with the initial loading direction, are referred to as "tensile half-loops" throughout the subsequent text. The half-loops that are below the slip axis are called "compression half-loops."

Table 4.1: The number of specimen replications in test samples.

Stud roughness at interface	Sample type				
	12% No-Gap	Green	18% Gap	12% Gap	12% Cycling
Smooth	24	19	13	11	24
Rough	25	24	11	12	25
Total	49	43	24	23	49

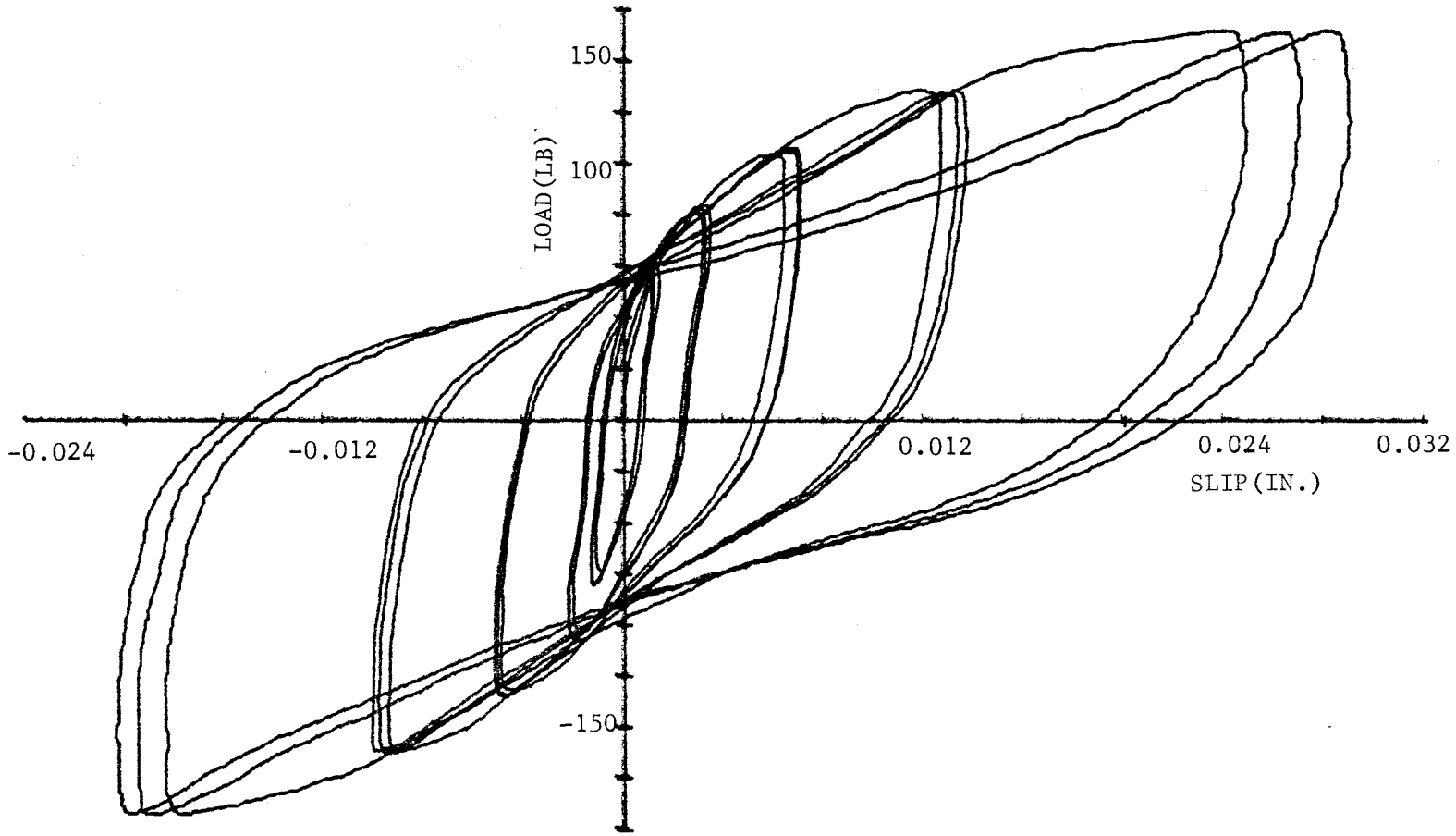

FIGURE 4.1 Typical L-S traces for samples without gap
(load levels are identified in Figure 3.7).

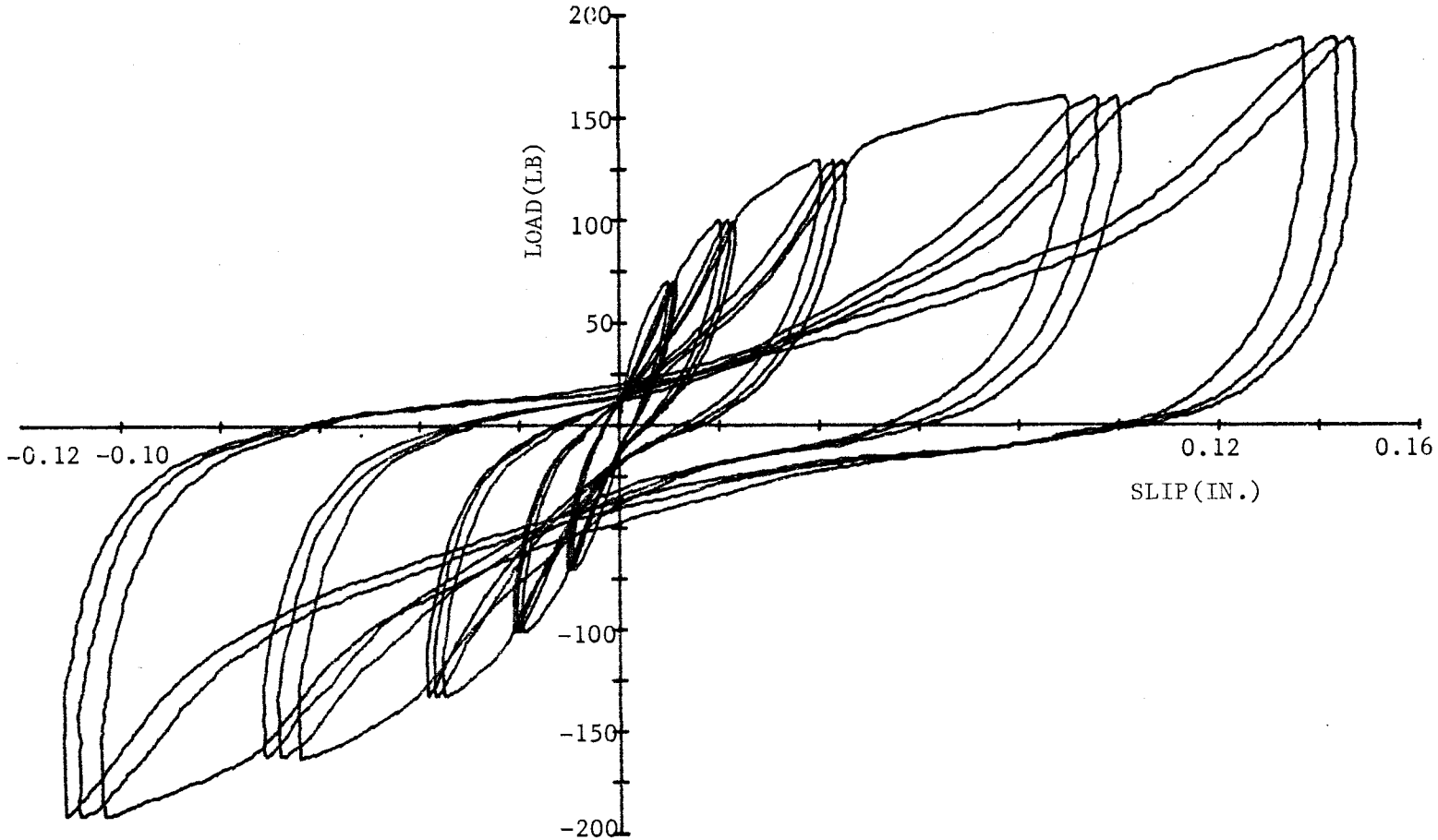

FIGURE 4.2 Typical L-S traces for samples with gap (load levels are identified in Figure 3.7).

The L-S traces are similar for samples without gap, and can be characterized by three typical regions (Fig. 4.1). In the first, identified as a softening region, the slope in loops between the load levels of 70 and 100 lb and -70 and -100 lb is decreasing with increasing load magnitude; that is, the joint stiffness is decreasing. In the second or transition region, the slope in loops at levels of 130 and -130 lb is rapidly changing and must be represented by several straight-line segments. The third is a hardening region between the loads of 160 and 190 lb and -160 and -190 lb, in which the slope between initial zero slip and the backbone curve is increasing; that is, the apparent joint stiffness gets larger under increasing load. (The backbone curve is a part of the load-slip relation that has slips larger than those achieved in the previous cycling.) The slope of the backbone trace decreases with the increasing load, which can be characterized as another region of joint softening.

Examples of this hardening and softening are the slopes in the first loops at load levels of 160 and 190 lb and -160 and -190 lb. The reason for softening at 70 and 100 lb load levels is the presence of the smaller sliding friction in the interlayer, which replaced the larger static friction. However, at 160 and 190 lb load levels, the softening is probably due to wood crushing under deforming nails. The hardening is probably caused by the nail bearing on dense wood that is produced by partial wood crushing in previous cycles. The decreasing slope of the backbone part of the trace is attributed to additional crushing of the wood under the nail.

Figure 4.2 illustrates the L-S traces of specimens with a drying-initiated gap between plywood and stud sections. Now, the initial

softening takes place sooner than for no-gap specimens of Figure 4.1, because the contact friction is absent. The gap prevents the friction and the shear force is transferred only by nail bearing on wood. Because of the rapid initial softening wood becomes crushed and the subsequent hardening becomes more pronounced than that of no-gap specimens.

4.2 Data Reduction

Among the three cycling loops at each load level, the first is a transition cycle between the lower- and current cycling load, the second is fully associated with the current cycling load, and the third is a transition cycle between the current- and the next-level cycling load (Fig. 4.1). Because the second loop was not directly affected by the cycling at the lower and higher loads, this loop was used to evaluate damping and stiffness. The L-S traces of the second loop were digitized by a computerized digitizer. The goal was to digitize a sufficient number of points on each trace to calculate the values of five dependent variables (DV) (Fig. 4.3): slip representation for tensile half-loops (OC), slip representation for compression half-loops (OF), total absorbed energy per loop (area AGBDHEA in Fig. 4.3), total energy capacity per loop (area OBCOEFO in Fig. 4.3), and damping ratio (Eq. (2.37)).

More than 100 points were digitized on each loop. To assure the accuracy of the digitized traces, more points were digitized in the highly curvilinear portions of the trace than in the linear portions (Fig. 4.3). The resulting mean and standard deviation of the five DV's at each testing condition are shown in Tables A1 through A8 of Appendix A.

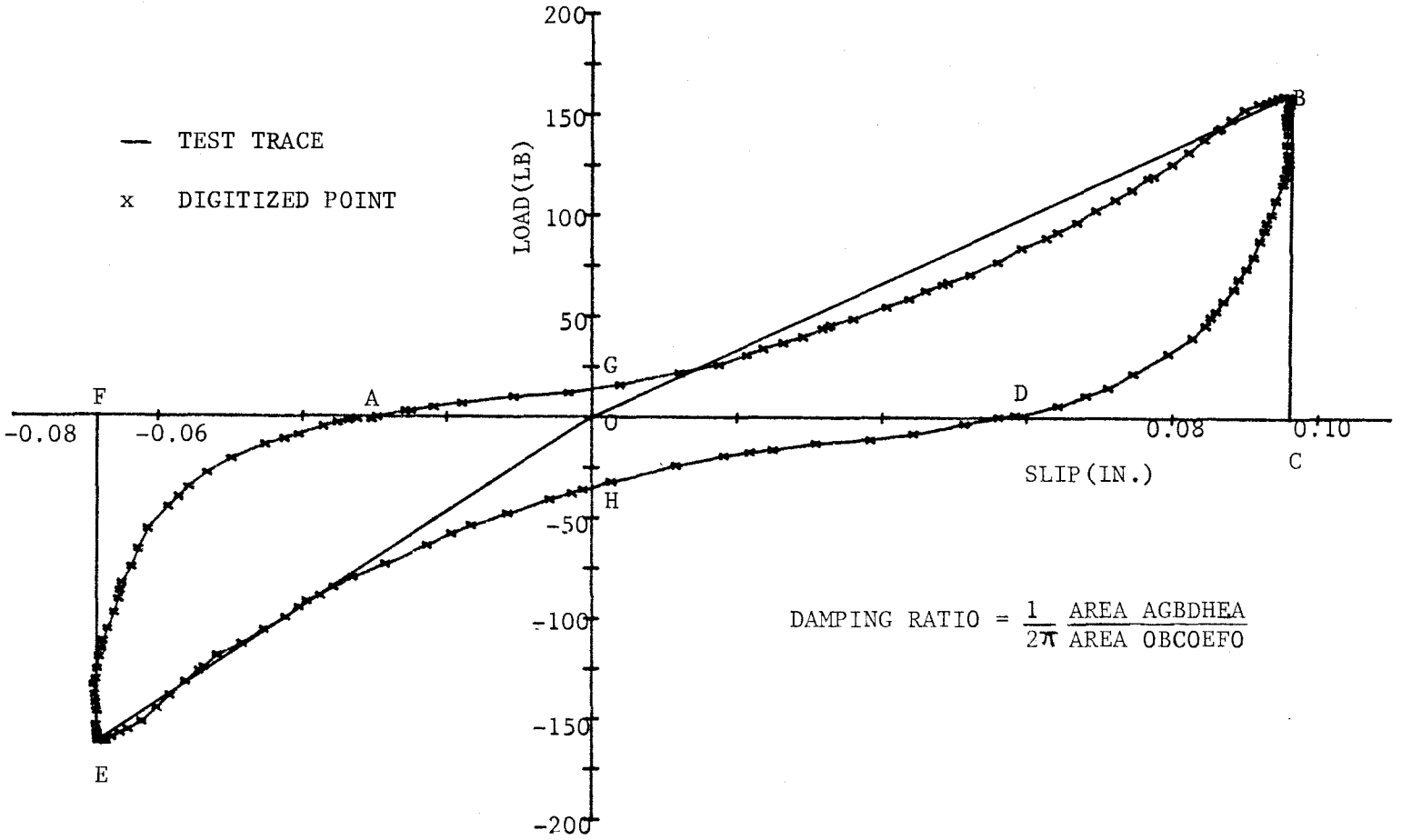

FIGURE 4.3 Typical digitized L-S trace of second loop at load level of 160 lb.

4.3 Data Analysis

Effects of MC, interlayer roughness, and load level on five DV's are evaluated and presented in this section. A standard program, Statistical Package for Social Science (SPSS) [15], was used in all the statistical analyses performed.

4.3.1 Combined Effects of All Variables

The first statistical analysis was a three-factor analysis of variance (ANOVA). The criterion for accepting the hypothesis is level of significance, α, for the variance ratio, F, which is defined as the ratio of explained variance (the variance between samples) and the unexplained variance (the variance within the samples). Table 4.2 shows the results: the critical significant level was set at one percent, so that the effect is significant if α is less than one percent.

The interaction between any two or more main effects, such as MC, load level and interlayer roughness, were examined first. If the interaction between two main effects was significant at one percent critical significant level, the analysis of either main effect was then conducted separately at every level of the other main effect. If only the main effect was significant and no significant interaction with others existed, then the analysis of the main effect was independent of the levels of other main effects; the subsequent analysis consisted of investigating each main effect with individual levels of other main effects. For example, the

Table 4.2: Significant level of F statistic for testing effects of moisture content, load level and interlayer roughness.

Sourse of Variation	Slip		Energy		Damping ratio
	tensile half-loops	compression half-loops	Absorbed	Capacity	
Main effects					
Moisture content (MC)	0.001*	0.001*	0.001*	0.001*	0.001*
Load level (LL)	0.001*	0.001*	0.001*	0.001*	0.001*
Interlayer roughness(ROU)	0.009*	0.894	0.099	0.052	0.001*
Interactions					
MCxLL	0.001*	0.001*	0.001*	0.001*	0.001*
MCxROU	0.565	0.001*	0.652	0.560	0.001*
LLxROU	0.068	0.998	0.400	0.185	0.827
MCxLLxROU	0.971	0.001*	0.825	0.594	0.999

* Significant at 1% critical significant level.

examination of slip of the tensile half-loop in Table 4.2 showed that a significant two-way interaction between MC and load level existed and that all the main effects were significant at one percent critical significant level. Thus, the analysis of MC effect on slip of the tensile half-loops was conducted at each load level (Section 4.3.2) and the effect of load level on this slip was conducted individually for the MC samples (Section 4.3.3). Since there was no significant interaction between interlayer roughness and other main effects, the interlayer roughness effect on the tensile slip was evaluated at an arbitrary level of other main effects (Section 4.3.4).

4.3.2 Effect of MC

The effect of MC on the slip of tensile half-loops, energy absorbed, energy capacity and damping ratio was evaluated at every load level separately by one-factor, variable MC, ANOVA tests at one percent critical significant level. The resulting α, which was always smaller than 0.01 at each load level, showed that MC significantly affects these four DV's. The same ANOVA tests were conducted on the slip of compression half-loops at all five load levels tested and at two conditions of interlayer roughness. The resulting α, which was also less than 0.01, indicated that the compression slip is significantly influenced by the MC.

It is postulated that the change in MC affects the stiffness, interface friction and nail bearing on wood in joints. High MC, such as that of Green Sample, is associated with a solid contact

between connected elements, which reduces the slip because of interlayer friction. Water saturation of the cell wall in specimens of the same sample, however, decreases the cell strength, which reduces the nail-bearing capacity and decreases joint stiffness. The reduction in MC of the joint lumber component produces a gap between the contact surfaces. The resulting loss of the frictional resistance to slip in these joints increases the slip. Therefore, the slip is larger in joints with gap than in those without it.

The investigation of the MC effect on the five DV's evaluated was conducted for the three combinations of samples: 12% No-Gap and 12% Cycling Samples for the effect of moisture cycling, 12% No-Gap, Green and 12% Cycling Samples for the effect of water saturation, Green, 18% Gap and 12% Gap Samples for the effect of drying-initiated gap. Figure 4.4 illustrates the effect of moisture cycling and water saturation on the slip of tensile half-loops and Figure 4.5 shows the relation between the gap and the tensile slip. Both coordinated the mean values of all the specimens in each sample tested. The relation between the MC and other four DV's is not shown graphically, because they displayed similar trends as evidenced by the analytical data presented in Tables A1 through A8 of Appendix A. The average MC of 12% No-Gap Sample was 12.6 percent, and 14.6 percent for 12% Cycling Sample (Appendix B). The Green Sample was assumed to be at the fiber saturation point of 28 percent MC.

The effect of MC on slip of tensile half-loops (TS) is examined next. Because TS in 12% Cycling Sample was smaller than

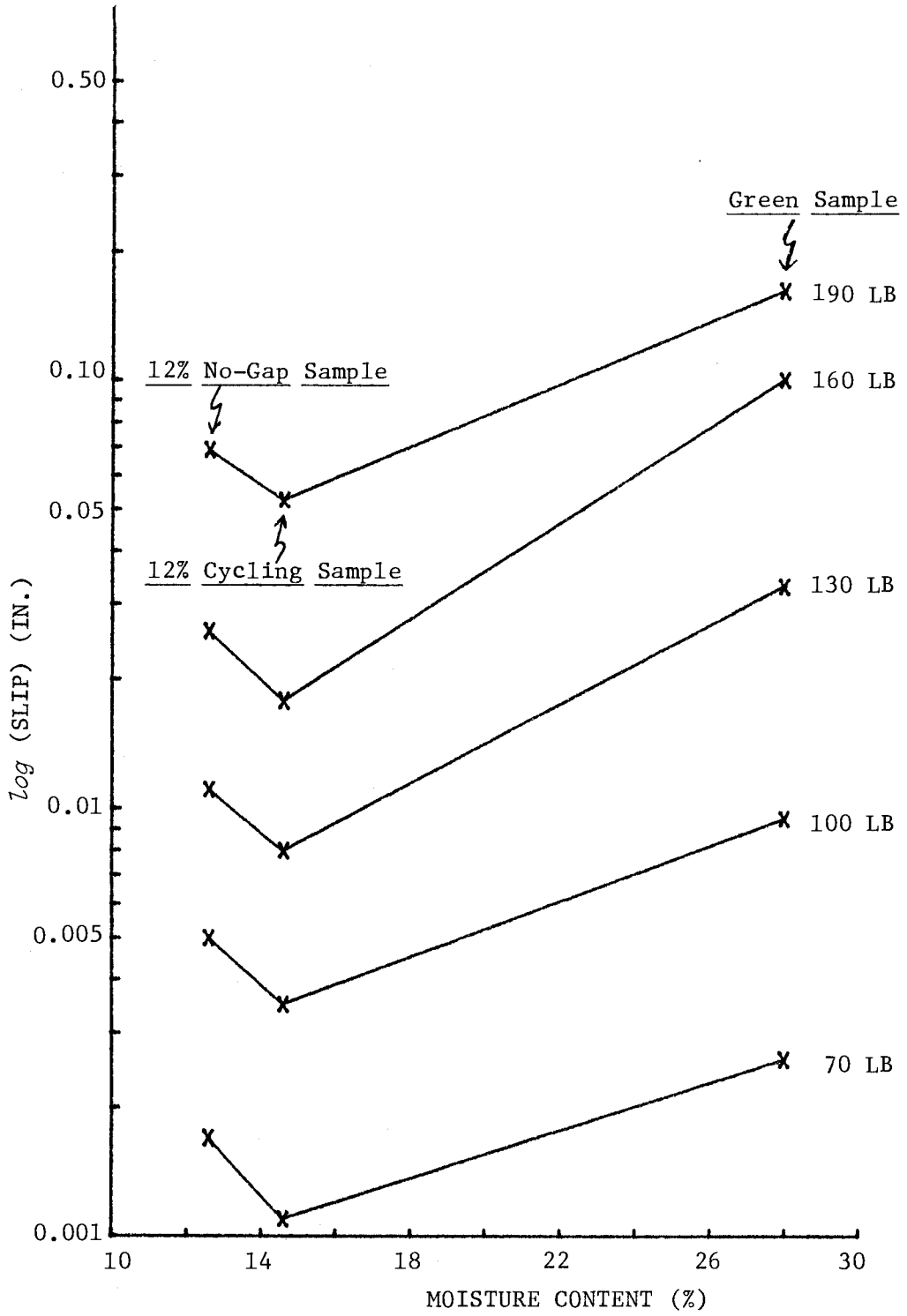

FIGURE 4.4 Relation between the MC and slip of tensile half-loops at tested load level for 12% No-Gap, Green and 12% Cycling Samples.

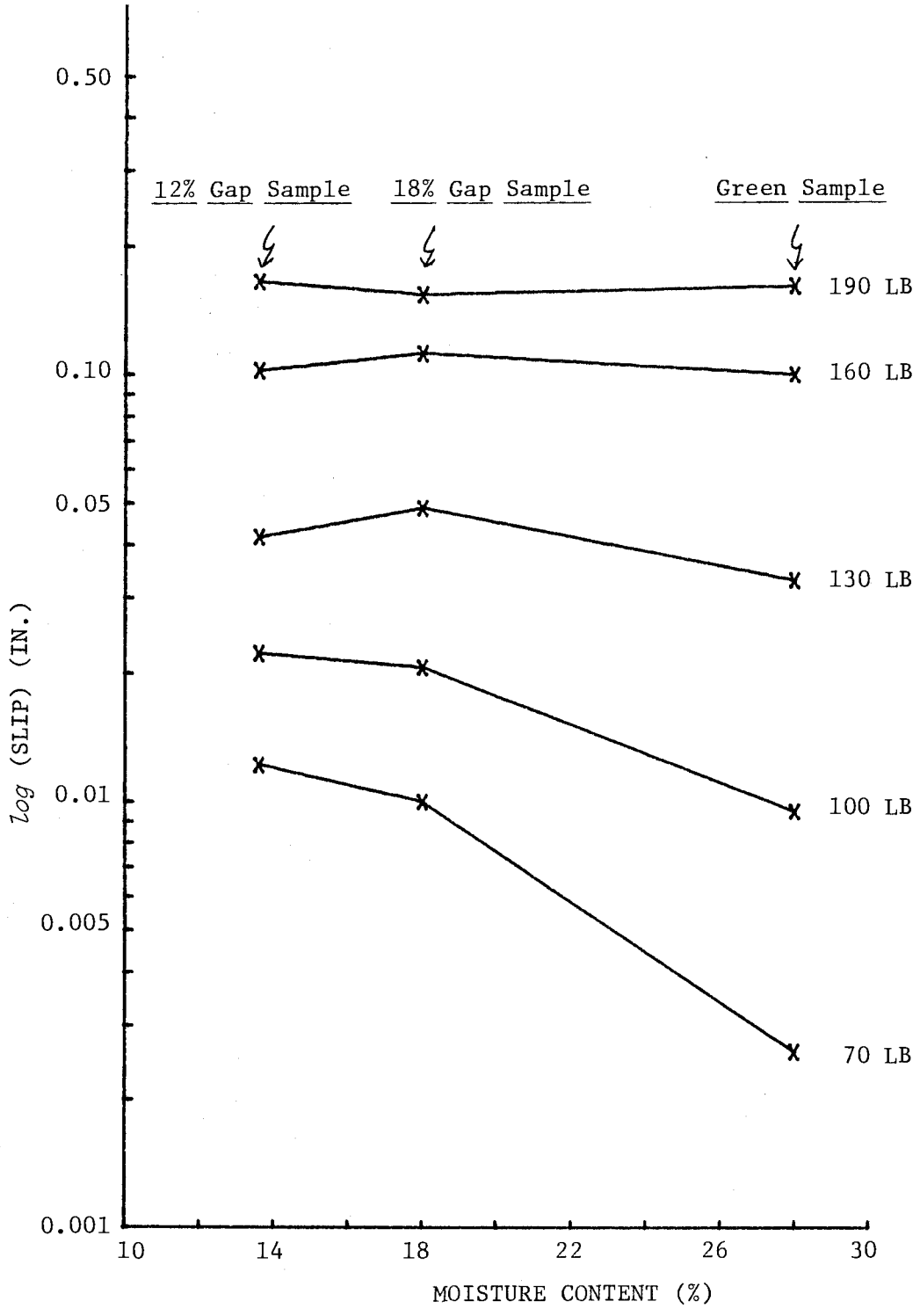

FIGURE 4.5 Relation between the MC and slip of tensile half-loops at tested load level for Green, 18% Gap and 12% Gap Samples.

that in 12% No-Gap Sample (Fig. 4.4), it appears that the moisture cycling in wood reduces the slip. This is probably due to the MC difference between 12% No-Gap and 12% Cycling Samples. In 12% Cycling Sample, higher MC of 14.6 percent at the end of cycling than the 12 percent at the time of specimen construction could have tightened the contact surfaces between the wood and plywood. This increased the friction and joint stiffness and reduced TS. In addition, TS of Green Sample is larger than that of 12% No-Gap and 12% Cycling Samples because of the larger strength of cell wall of the drier samples. Another reason may be the lubricating effect of the water trapped in the interlayer of the Green Sample. This decreases the contact friction and increases the slip.

The gap effect on TS is illustrated by observing that TS of samples with gap is larger than that of Green Sample (Fig. 4.5). The reason for this observation may be the dominating effect of interlayer gap over the strength effect on wood cell wall.

Next, the MC effect on slip of compression half-loops (CS) is discussed. For joints with smooth interface, moisture cycling caused smaller CS in 12% No-Gap Sample than in 12% Cycling Sample. Among the joints with rough interface, specimens in 12% No-Gap Sample had a larger CS than those in 12% Cycling Sample. This could be attributed to the fact that the CS reduction due to interlayer friction is smaller than the CS increase due to nail bearing on wood in joints with rough interface. CS of Green Sample is larger than that of 12% No-Gap or 12% Cycling Samples. The small CS of joints with rough interface in Green Sample at

load level of 70 lb (Table A2) is probably due to large data variability and more replications would be needed to explain this variation. The final observation in this category pertains to CS of samples with gap which is larger than that of samples without gap (Table A2).

The following discussion illustrates the effect of MC on the total energy absorbed per loop (EA). The magnitude of EA depends on the slip, load level, and the shape of load-slip, L-S, trace as expected, because this energy is the area under the trace. Moisture cycling of lumber in joints before testing somewhat increases EA as observed by comparing 12% No-Gap and 12% Cycling Samples (Table A7). This is probably due to the friction that dominates the changes in nail bearing, which is supported by observing that the slip at corresponding loads of 12% No-Gap Sample is close to that of 12% Cycling Samples. Green Sample has larger EA than 12% No-Gap and 12% Cycling Samples. The reason could be a negligible friction force, as indicated by much larger slip of Green Sample than that of 12% No-Gap Sample (Table A6).

The effect of drying-initiated gap on EA is discussed by comparing Green, 18% Gap and 12% Gap Samples. At load levels of 70 and 100 lb, all the samples with gap have larger EA than Green Sample (Table A7), because they have larger slips and areas under L-S traces than Green Sample. However, at load levels above 100 lb, EA of Green Sample becomes larger than that of samples with gap, because the frictional shear force is present in Green Sample but not in the samples with gap and slips at loads above 100 lb

are about the same for the three samples (Table A6).

The discussion below concerns the MC effect on the total energy capacity per loop (EC). As expected, EC increases as the load and slip get larger (Table A7). For 12% Cycling Sample, EC is smaller than 12% No-Gap Sample, because the slip and areas under loops decrease as the result of moisture cycling. Green Sample has larger EC than either 12% No-Gap or 12% Cycling Samples due to increased slip caused by weaker cell wall strength in water-saturated lumber. Samples with gap have larger EC than Green Sample (Table A7) because of larger slips and associated areas under L-S loops.

The MC effect on damping ratio (DR) is most important in this investigation. The results show that DR of joints is dominated by the interlayer friction. Moisture cycling in stud section increases DR, as indicated by larger DR of 12% Cycling Sample than that of 12% No-Gap Sample. The possible reason is the large energy dissipated by the tighter interlayer at 14.6 percent MC in 12% Cycling Sample as compared to the not-so-tight interlayer of 12% No-Gap Sample at about 12 percent (Table A5). Green Sample has larger DR than 12% No-Gap Sample but a smaller one than 12% Cycling Sample. A possible explanation is the water pockets trapped in interfaces of joints in water-saturated Green Sample, which is discussed earlier in the text.

The final observation on DR pertains to joints with rough interfaces. For Green Sample at load levels of 100 and 130 lb, these joints have DR larger than 12% Cycling Samples. The possible

explanation includes previously discussed tightening of the interface and associated larger friction of Green Sample than those of 12% Cycling Sample. Table A5 also shows that samples with gap have DR smaller than that of samples without gap.

4.3.3 Effect of Load Level

One-factor analysis (ANOVA) was conducted at one percent critical significant level for five MC samples to examine the effect of the load on the four dependent variables: slip of tensile half-loops (TS), energy absorbed (EA), energy capacity (EC) and damping ratio (DR). The resulting α, which is smaller than 0.01, indicates that the load level does influence all four variables. For slip of compression half-loops (CS), the test of significance was conducted for all five MC samples and at both interlayer roughness used in this study. Like in TS, the results show that significant influences exist.

Figures 4.6 to 4.10 illustrate the relation between the load level and variables TS, CS, EC and EA. As expected, all the graphs consistently display increased slip, energy absorbed and energy capacity with increased load. These increases are the least for 12% No-Gap and 12% Cycling Samples, because of large interlayer friction and nail bearing on stronger drier wood. Both these effects gets smaller as the load gets larger because of load-produced gap. Under increasing loads, these specimens are gradually becoming similar to the corresponding specimens with the drying-produced gap. AT load levels of 70 and 100 lb, TS, CS, EA, and EC of Green Sample are similar to those of 12% No-Gap and 12%

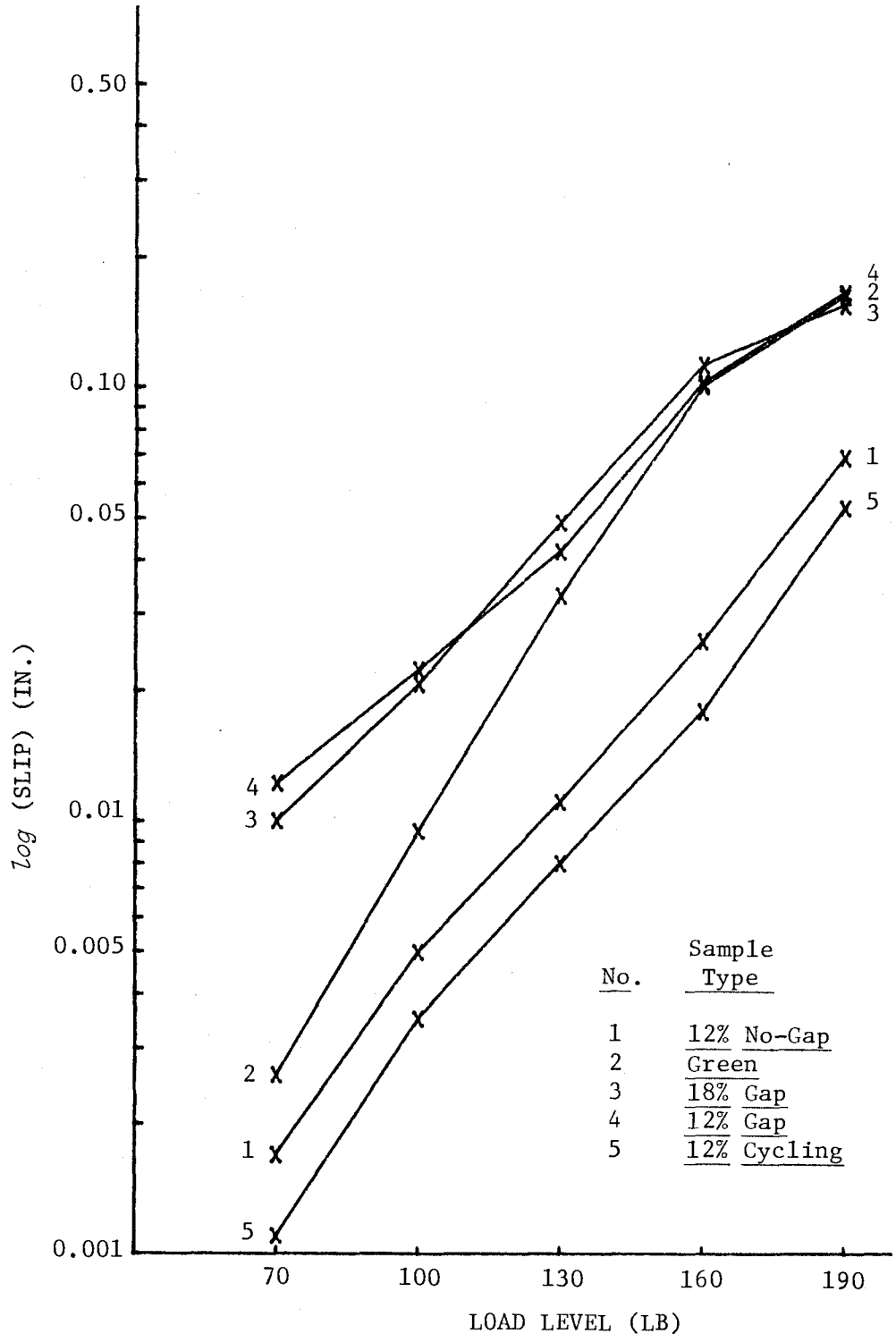

FIGURE 4.6 Relation between the load and slip of tensile half-loops for five MC samples investigated.

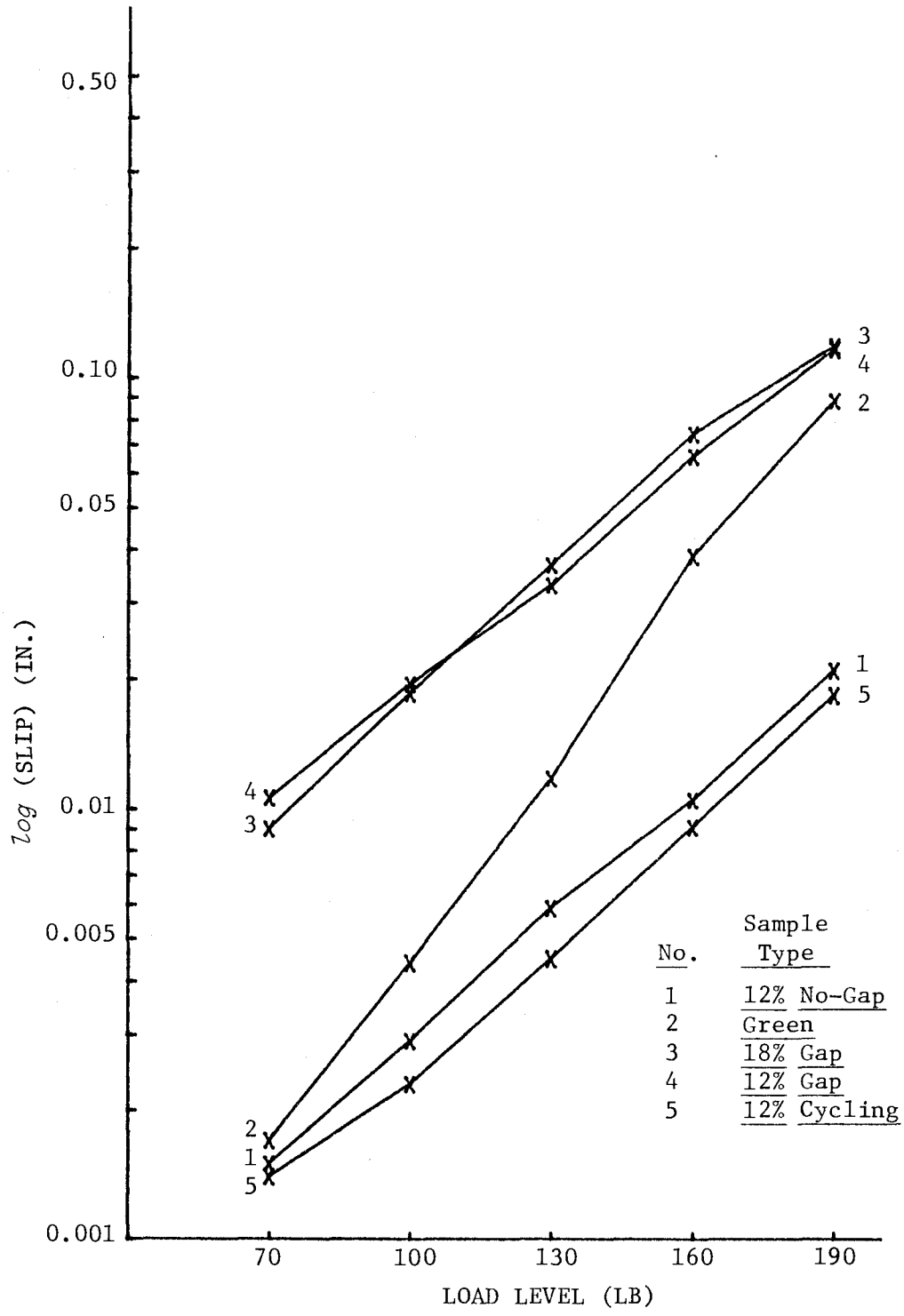

FIGURE 4.7 Relation between the load and slip of compression half-loops for five MC samples with smooth interface.

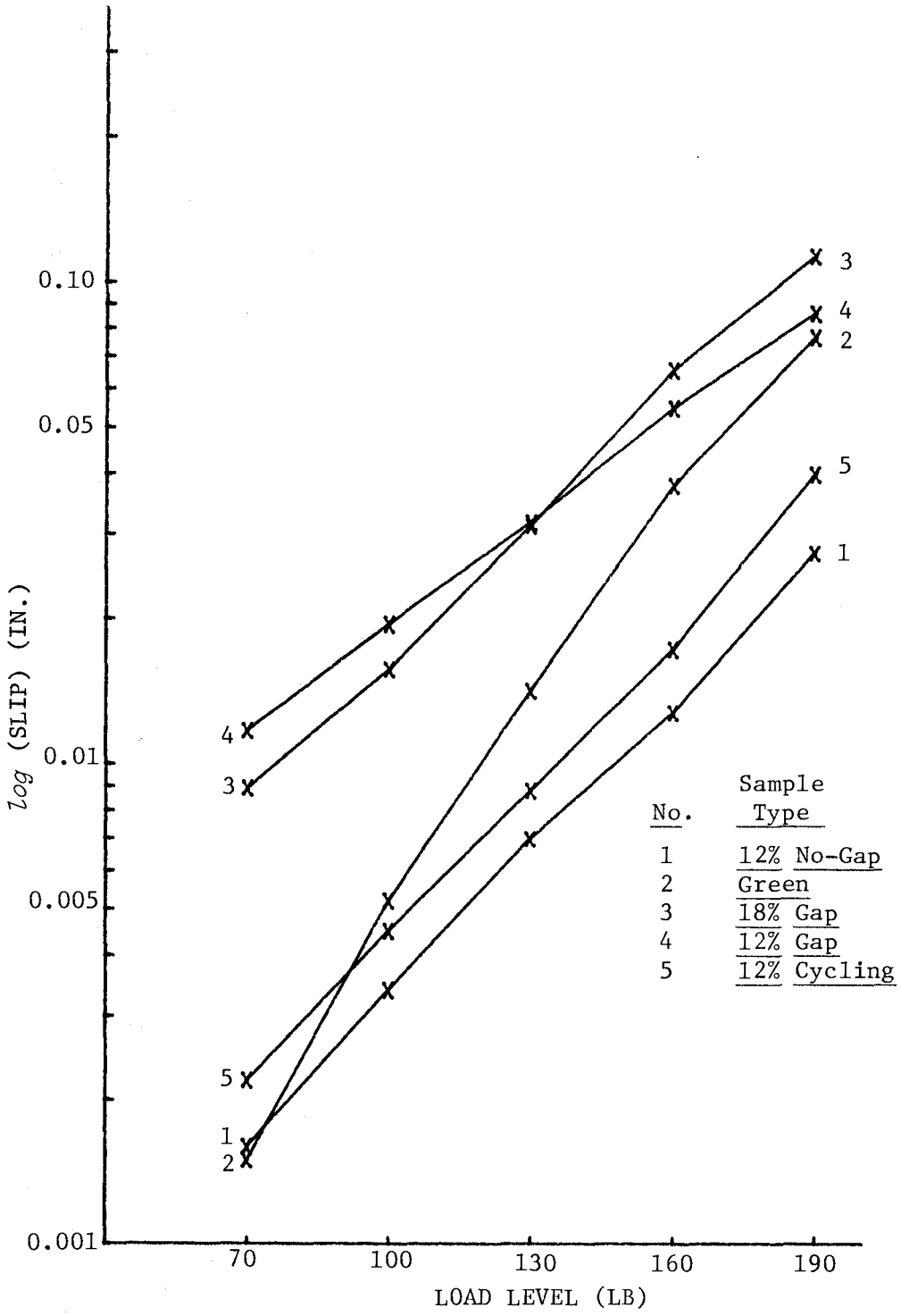

FIGURE 4.8 Relation between the load and slip of compression half-loops for five MC samples with rough interface.

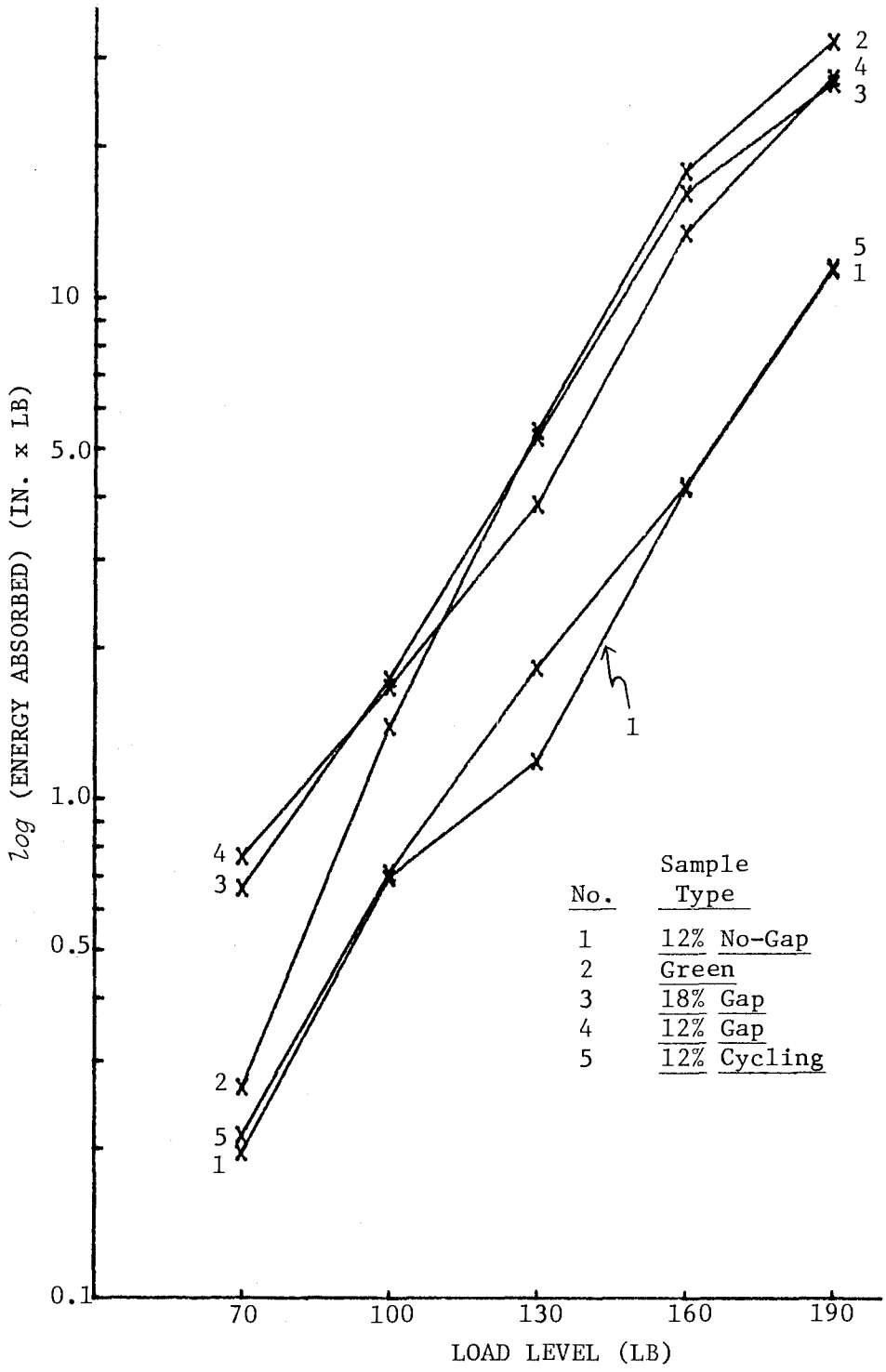

FIGURE 4.9 Relation between the load and total energy absorbed per loop for five MC samples investigated.

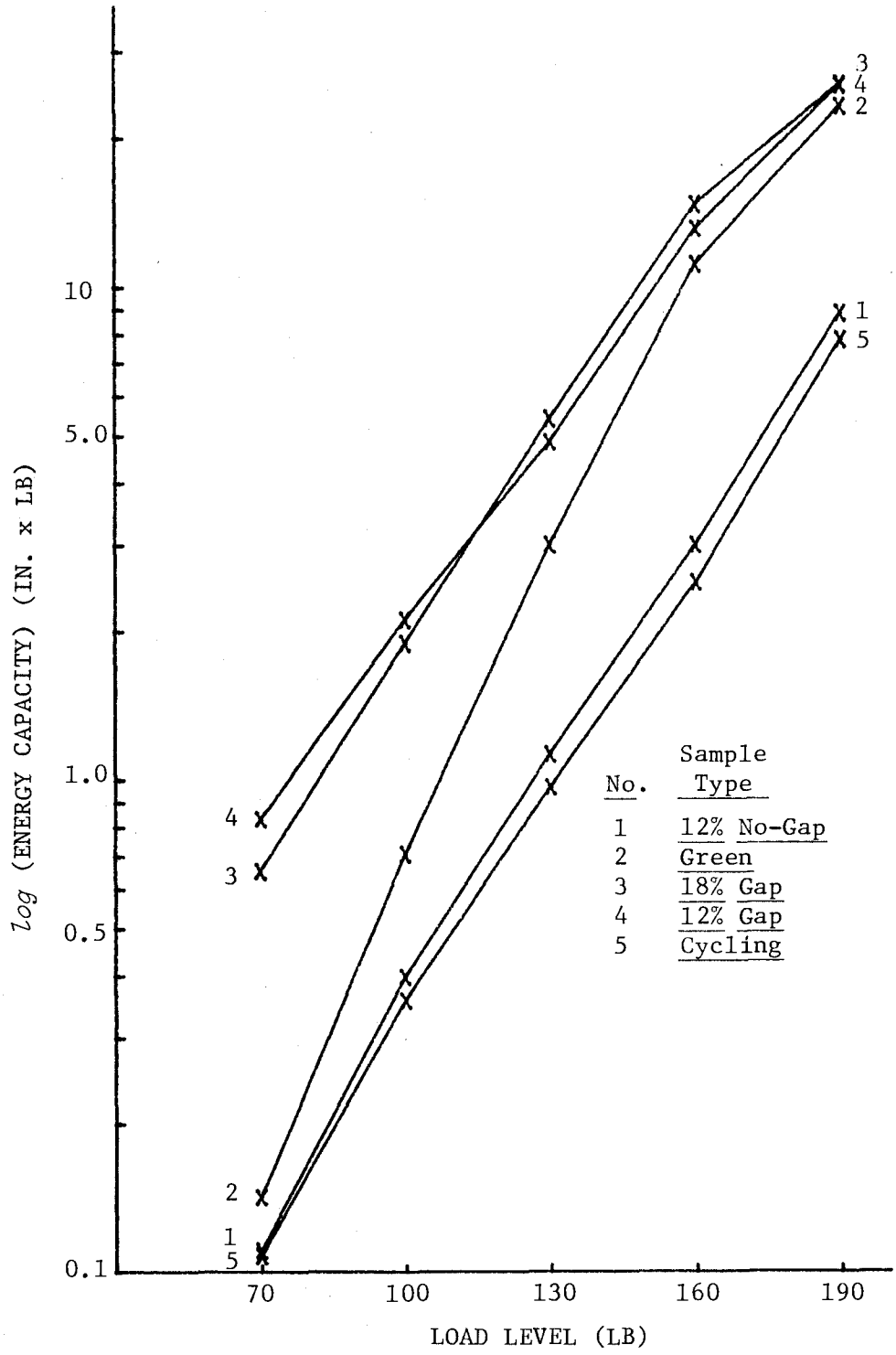

FIGURE 4.10 Relation between the load and total energy capacity per loop for five MC samples investigated.

Cycling Samples. At increased loads, the variables of Green Sample approach those of the samples with gap. This observation can be explained by the interlayer friction at small loads of specimens without gap. Similar reasoning suggests that the weaker cell wall in lumber and associated nail bearing strength in Green Sample produce slip increases at high load.

Figure 4.11 illustrates the relation between DR and load level for all five MC samples. Samples without gap have DR getting smaller under increasing load, but it gets larger in samples with gap. It is interesting to notice that DR of Green Sample decreases at all increasing loads except at 70 lb. Again, DR of 12% Gap Sample increases at all increasing load except at 70 lb. The most likely explanation is the appearance of a partial gap at high load when the plywood section is pulled apart from lumber, thus breaking the interface. The result is the reduced friction and damping. However, for joints with initial gap as the result of moisture cycling, high load could have partially closed the gap, because of nail bending. The result is partial interface friction and larger damping.

Figure 4.11 shows the reduction of DR for 18% Gap Sample at 190 lb, which is just the opposite from the observation for other loads and samples. However, the reduction was small and could be attributed to the data variation. A larger sample size than the one used in this study would be needed to detect if the reduction is significant.

The relations between the load and all five DV's were

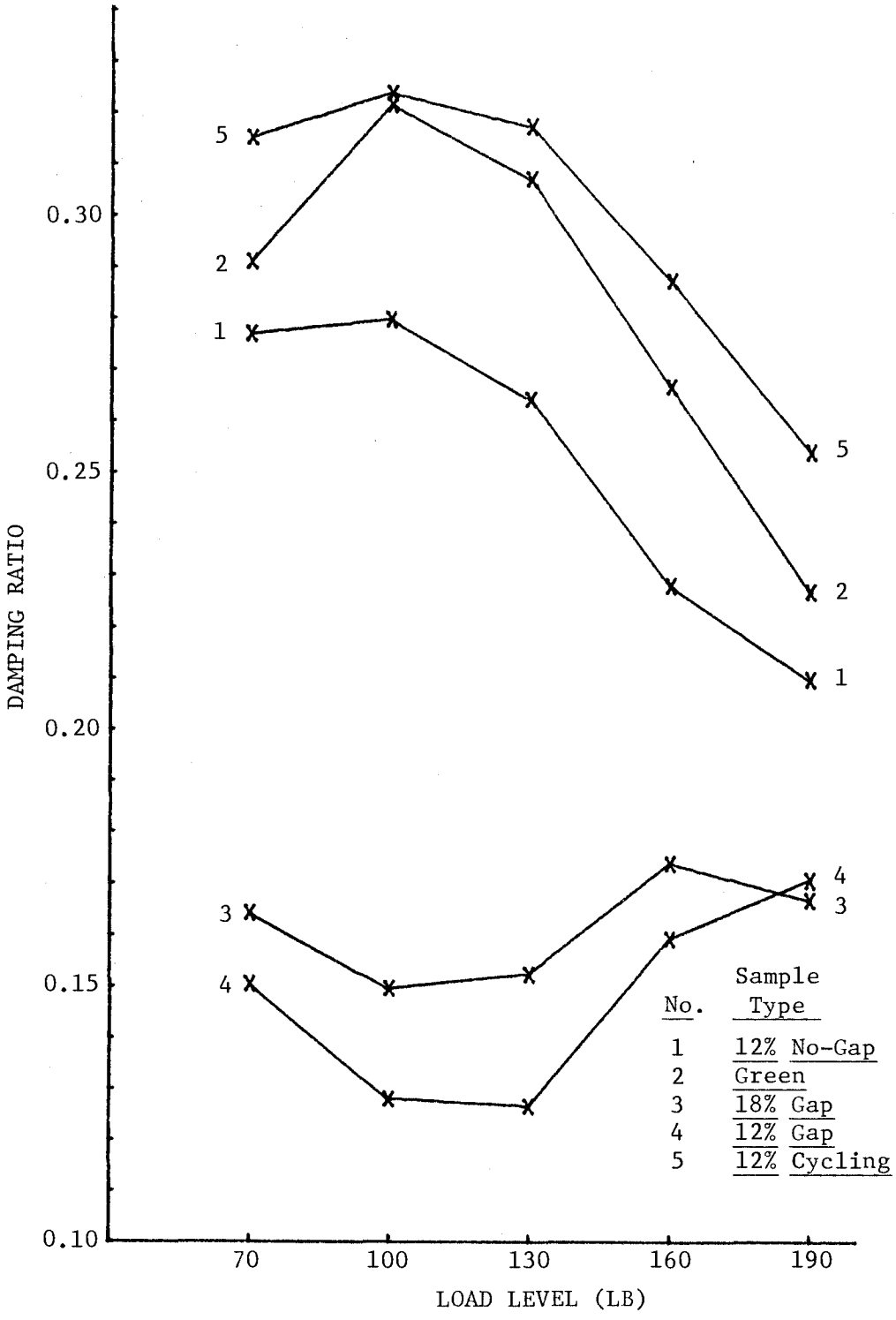

FIGURE 4.11 Relation between the load and damping ratio for five MC samples investigated.

investigated by performing linear regression analysis using the following model:

$$Y = A + B * LL + C * AMC \qquad (4.1)$$

where LL = load levels of 70, 100, 130, 160 or 190 lb,

AMC = estimated MC of lumber (12.6 percent for 12% No-Gap Sample, 28 percent for Green Sample, 18 percent for 18% Gap Sample, 13.6 percent for 12% Gap Sample and 14.6 percent for 12% Cycling Sample), and

A, B and C = regression constants.

Four sets of samples were analyzed, which were matched as in Figures 4.6 through 4.11. The first two sets deal with TS, CS, EA and EC; one consists of Green, 18% Gap and 12% Gap Samples and the other of 12% No-Gap, Green and 12% Cycling Samples. Additional two sets are concerned with DR: one consists of 18% Gap and 12% Gap Samples and the other of 12% No-Gap, Green and 12% Cycling Samples. Table 4.3 lists the resulting constants, A, B and C, of each regression equation and coefficient of determination, R^2. The value for R^2 of TS, CS, EA and EC is consistently above 0.7, which is well above the value of 0.5, which is the value usually associated with the widely accepted correlation between modulus of elasticity and modulus of rupture for lumber. However, the values for R^2, associated with DR, are smaller, which means the testing in this study has not revealed a strong correlation between DR and load level and MC.

Table 4.3: Regression equations defining the effect of load level and moisture content on joint properties.

Dependent Variable Y*	Matched samples**	Regression model: Y=A+B*LL+C*AMC A	B	C	R^2
LOG(TS)	2,3,4	1.2967	0.01273	-0.02041	0.84690
LOG(CS)		1.5581	0.01168	-0.03722	0.80561
LOG(EA)		0.6661	0.01577	-0.0442	0.90927
LOG(EC)		1.0037	0.01592	-0.02566	0.91001
LOG(TS)	1,2,5	-0.3498	0.01411	0.03089	0.82569
LOG(CS)		-0.0371	0.01138	0.02022	0.73535
LOG(EA)		-0.2433	0.01566	0.02794	0.90246
LOG(EC)		-0.5654	0.01655	0.02648	0.90206
DR	3,4	788.9	34.17	1.63	0.09806
DR	1,2,5	3728.6	-5.51	0	0.09862

* TS: slip (x10,000) for tensile half-loops,
CS: slip (x10,000) for compression half-loops,
EA: total energy absorbed (x100) per loop,
EC: total energy capacity (x100) per loop,
DR: damping ratio (x10,000).

** Sample type : 1: 12% No-Gap,
2: Green,
3: 18% Gap,
4: 12% Gap,
5: 12% Cycling.

4.3.4 Effect of Interface Roughness

The discussion of interlayer roughness is restricted to the samples without gap (12% No-Gap, Green and 12% Cycling Samples), because the interlayer gap (18% Gap and 12% Gap Samples) physically prevents the interlayer friction, thus nullifying the possibility of roughness contribution to joint behavior.

In general, TS of joints with smooth interface is smaller than that of joints with rough interface (Table A1). In rough specimens, summerwood of lumber is in touch with the summerwood of plywood, while in smooth specimens both, summerwood and springwood parts of the contact surfaces are in touch. Therefore, the friction between the two dense summerwood surfaces of rough joints is smaller than that between the two softer mixed surfaces of soft specimens. This observation is contradicted by Green Sample which has larger TS for smooth interface than for rough interface. Again, water trapped in the interlayer could have lubricated the contact surfaces and change the friction mechanism.

Additional effects were investigated by one-factor ANOVA statistical package at one percent critical significant level. All the load and MC levels were included to examine the influence of interlayer roughness on the slip of compression half-loops. The results showed that types of interface roughness consistently tested the same (Table 4.4). Therefore, it can be concluded that the two types of interfaces investigated were not that much different.

Table 4.4: Significant level of F ratio for testing effect of interface roughness on slip of compression half-loops.

	Sample type				
Load level (lb)	12% No-Gap	Green	18% Gap	12% Gap	12% Cycling
70	0.8640	0.6512	0.4137	0.1918	0.3316
100	0.7727	0.9192	0.5384	0.1711	0.0792
130	0.4107	0.8734	0.2983	0.2784	0.2035
160	0.3778	0.4130	0.1143	0.1586	0.2639
190	0.4222	0.7148	0.8807	0.2878	0.3889

Interface roughness investigated shows no significant effect on EA and EC at five percent critical significant level (Table 4.2). However, the comparison of the means for EA and EC at each MC and load level of 12% No-Gap and 12% Cycling Samples (Tables A3 and A4) shows that both types of energy are always smaller in smooth interfaces than those in rough interfaces. The reason is the smaller slip in joints with smooth interfaces, as discussed before. However, specimens of Green Sample with smooth interface again display smaller EC and EA than those with rough interface at all load levels except at 70 and 190 lb. The reason is that of the already discussed water lubrication.

Factors that influence the damping ratio (DR) have the greatest practical importance. The interlayer roughness effect on DR was conducted at one percent critical significant level by ANOVA package for all MC samples. As expected, the samples without gap show that interface roughness significantly influences DR (Table 4.5). For 12% No-Gap and 12% Cycling Samples, this ratio is larger in joints with smooth interface than that for joints with rough interface. Again, the reason is the larger frictional force presented in smooth-interface joints. However, the influence of interlayer roughness on DR is insignificant in Green Sample. Again, the explanation is the water lubrication.

4.4 Practical Impact and Application

In general, the results of this investigation characterize the effect of loading, moisture content and joint-interlayer

Table 4.5: Comparison of damping ratio between joints with rough and smooth interface

Statistics	Sample type				
	12% No-Gap	Green	18% Gap	12% Gap	12% Cycling
Significant level of F ratio	0.0039	0.8312	0.2328	0.0494	0.0003
DR in smooth-interface joint					
Mean	0.2611	0.2852	0.1584	0.1526	0.3170
Standard deviation	0.0431	0.0552	0.0255	0.0357	0.0763
Sample size	118	86	65	55	117
DR in rough-interface joint					
Mean	0.2440	0.2835	0.1652	0.1404	0.2844
Standard deviation	0.0477	0.0522	0.0353	0.0288	0.3003
Sample size	122	111	50	57	122

condition on slip, energy absorption and damping ratio of one-nail joint specimens between 19/32-in. plywood and Douglas-fir lumber. The most significant result is the reduction of stiffness and damping ratio of joints that are consturcted with green lumber and then dried to the service moisture content level. Because most joint tests presently neglect the drying effects, the results can introduce an overestimate of the composite stiffness when used in the evaluation of the structural behavior of wood components. Therefore, the joint stiffness and damping should include the effects of drying after assembly. It is anticipated that correction factors can be developed to correct the test data for such effects.

V. CONCLUSIONS AND RECOMMENDATIONS

The most important conclusions reached for nail joints tested in this investigation are the following:

1. A two percent MC increase of lumber at 12% No-Gap Sample results in about 1.17 times stiffer joints with 1.19 times larger damping;
2. Drying-initiated gap reduces stiffness and damping ratio of joints that are constructed of green lumber and dried afterwards;
3. Joints constructed and tested with dry lumber are at least three times stiffer than joints constructed with green lumber which are dried afterwards;
4. Damping ratio decreases with increasing load for joints that are constructed and tested dry, but increases with increasing load for joints that are constructed green and tested dry;
5. Joints with smooth interface are about 1.14 times stiffer and have about 1.06 times larger damping ratio than those with rough interface; and
6. The slip, energy absorbed and energy capacity increase with increasing load.

The following recommendations were derived from the results of this study:

1. Cyclic-load instead of free-vibration test is recommended for future testing of single-nailed joints;

2. Additional tests are recommended to define the relation between the change of moisture content and gap size more accurately; and
3. An investigation is also recommended to evaluate correction factors for changes in moisture content of commonly found joints.

BIBLIOGRAPHY

[1] American Society for Testing and Materials. Annual Book of Standards, Vol. 4, No. 9. Wood, Philadelphia, PA 19103, 1983.

[2] Antonides, C. E., M. D. Vanderbilt and J. R. Goodman. "Interlayer Gap Effects on Nail Slip Modulus." Structural Research Report No. 22. Colorado State University, Ft. Collins, Colorado, March, 1979.

[3] Atherton, George H., Kenneth E. Rowe and Ken M. Bastendorff. "Damping and Slip of Nailed Joints." Wood Science, Vol. 12, No. 4, April, 1980, pp. 218-226.

[4] Atherton, George H. and Stanley E. Corder. "Human Response to Vibration of Floors in Occupied Dwellings." Forest Products Journal, Vol. 29, No. 7, July, 1979, pp. 29-38.

[5] Earles, S. W. and M. G. Philpot. "Energy Dissipation at Plane Surfaces in Contact." Journal of Mechnical Engineering Science, Vol. 9, No. 2, 1967, pp. 86-97.

[6] Jacobsen, Lydik S. and R. S. Ayre. Engineering Vibrations, with Applications to Structures and Machinery." McGraw Hill, New York, 1958.

[7] James, William L. "Effect of Temperature and Moisture Content on Internal Friction and Speed of Sound in Douglas-fir." Forest Products Journal, Vol. 11, No. 9, September, 1961, pp. 383-390.

[8] Keneta, K. "Study of Structural Damping and Stiffness in Nailed Joints." Engineer's Thesis, Stanford University, 1958.

[9] Kimball, A. L. and D. E. Lovell. "Internal Friction in Solids." Physical Review, Second Series, Vol. 30, 1927, pp. 948-957.

[10] Kollmann, F. and H. Krech. "Dynamische Messung der Elastischen Holzergenschaften and Dampung." Holz als Roh-und Werkstoff, Vol. 18, No. 2, 1960, pp. 4-54.

[11] Lazan, Benjamin J. Damping of Materials in Structural Mechanics. Pergamon Press, Inc., Great Britain, 1968.

[12] Loferski, Joseph R. "Inelastic Stiffness Moduli for Nail Joints between Wood Studs and Plywood Sheathing." M.S. Thesis, Department of Forest Products, Oregon State University, Corvallis, Oregon, 1980.

[13] Matsumotom, Tsutomu. "Studies on the Dynamic Modulus E and the Logarithmic Decrement of Wood by Transverse Vibration." Bulletin of the Kyushu University Forests, No. 36, November, 1962.

[14] Medearis, Kennth. "An Investigation of the Static and Dynamic Characteristics of Shear Wall Structure." 831, Piper Avenue, Sunnyvale, CA, February, 1966.

[15] Nie, Norman H. et al. SPSS-Statistical Package for the Social Sciences, second edition. McGraw Hill, New York, 1975.

[16] Polensek, A. "Damping Capacity of Nailed Wood-Joist Floors." Wood Science, Vol. 8, No. 2, October, 1975, pp. 141-151.

[17] Polensek, A. "Damping of Roof Diaphragms with Tongue-and-Groove Decking." Wood Science, Vol. 9, No. 2, October, 1976, pp. 70-77.

[18] Polensek, A. "Static and Dynamic Properties of Glued Wood-Joist Floors." Forest Products Journal, Vol. 21, No. 12, December, 1971, pp. 31-39.

[19] Polensek, A. "Human Response to Vibration of Wood-Joist Floor System." Wood Science, Vol. 3, No. 2, October, 1970, pp. 111-119.

[20] Robertson, J. M. and A. J. Yorgiadis. "Internal Friction in Engineering Materials." Journal of Applied Mechanics, Vol. 68, September, 1946, pp. A173-A182.

[21] Wilkinson, Thomas L. "Vibrational Loading of Mechanically Fastened Wood Joints." Forest Products Journal, No. 274, USDA FS Forest Products Laboratory, Madison, Wisconsin, 1976.

[22] Yeh, C. T., B. J. Hartz and C. B. Brown. "Damping in Glued and Nailed Wood Structures." Journal of Sound and Vibration, Vol. 19, No. 4, November, 1970, pp. 411-419.

[23] Yeh, C. T. "A Study on the Mechniams of Damping in Wood Structures." Ph.D. Thesis, Department of Civil Engineering, University of Washington, 1970.

[24] Young, D. H. and K. Medearis. "An Investigation of the Structural Damping Characteristics of Composite Wood Structures Subjected to Cyclic Loading." Department of Civil Engineering, Stanford University, Palo Alto, CA, 1962.

APPENDICES

APPENDIX A

STATISTICS FOR VARIABLES INVESTIGATED

Table A1: Statistics for slip of tensile half-loops.

Sample type	Load level (lb)	Smooth-interface (in.) N	Mean	Standard deviation	Rough-interface (in.) N	Mean	Standard deviation
12% No-Gap	70	24	0.0017	0.0009	24	0.0017	0.0008
	100	24	0.0049	0.0018	25	0.0050	0.0022
	130	24	0.0105	0.0034	25	0.0116	0.0050
	160	24	0.0243	0.0105	25	0.0276	0.0147
	190	22	0.0636	0.0415	23	0.0739	0.0435
Green	70	17	0.0028	0.0022	23	0.0025	0.0018
	100	19	0.0096	0.0074	23	0.0094	0.0051
	130	17	0.0339	0.0339	23	0.0326	0.0174
	160	16	0.0926	0.0578	23	0.1063	0.0454
	190	17	0.1595	0.0574	19	0.1650	0.0284
18% Gap	70	13	0.0104	0.0026	10	0.0095	0.0024
	100	13	0.0213	0.0049	10	0.0200	0.0051
	130	13	0.0443	0.0123	11	0.0541	0.0304
	160	13	0.0995	0.0324	11	0.1280	0.0517
	190	13	0.1537	0.0391	8	0.1564	0.0395
12% Gap	70	11	0.0115	0.0027	12	0.0129	0.0025
	100	11	0.0208	0.0047	12	0.0237	0.0052
	130	11	0.0388	0.0116	12	0.0445	0.0127
	160	11	0.0893	0.0345	12	0.1146	0.0470
	190	11	0.1565	0.0382	9	0.1766	0.0439
12% Cycling	70	24	0.0010	0.0006	25	0.0012	0.0008
	100	24	0.0030	0.0010	25	0.0039	0.0020
	130	24	0.0073	0.0029	25	0.0087	0.0047
	160	23	0.0162	0.0079	24	0.0195	0.0120
	190	22	0.0468	0.0311	23	0.0583	0.0542

Table A2 : Statistics for slip of compression half-loops*.

Sample type	Load level (lb)	Smooth-interface (in.) Mean	Smooth-interface (in.) Standard deviation	Rough-interface (in.) Mean	Rough-interface (in.) Standard deviation
12% No-Gap	70	0.0015	0.0011	0.0016	0.0008
	100	0.0029	0.0021	0.0034	0.0018
	130	0.0059	0.0039	0.0070	0.0037
	160	0.0105	0.0059	0.0128	0.0068
	190	0.0210	0.0129	0.0274	0.0162
Green	70	0.0017	0.0015	0.0015	0.0012
	100	0.0044	0.0034	0.0052	0.0032
	130	0.0118	0.0075	0.0142	0.0079
	160	0.0386	0.0199	0.0378	0.0182
	190	0.0886	0.0319	0.0768	0.0338
18% Gap	70	0.0090	0.0024	0.0089	0.0021
	100	0.0186	0.0044	0.0157	0.0055
	130	0.0368	0.0113	0.0312	0.0109
	160	0.0742	0.0233	0.0656	0.0239
	190	0.1185	0.0296	0.1131	0.0260
12% Gap	70	0.0106	0.0028	0.0117	0.0028
	100	0.0195	0.0043	0.0195	0.0042
	130	0.0330	0.0066	0.0317	0.0075
	160	0.0658	0.0200	0.0548	0.0145
	190	0.1165	0.0363	0.0861	0.0206
12% Cycling	70	0.0014	0.0007	0.0022	0.0018
	100	0.0023	0.0015	0.0045	0.0047
	130	0.0045	0.0027	0.0088	0.0080
	160	0.0091	0.0057	0.0173	0.0144
	190	0.0184	0.0123	0.0399	0.0363

* Sample sizes are the same as in Table A1.

Table A3 : Statistics for total energy absorbed per loop*.

Sample type	Load level(lb)	Smooth-interface(in.xlb) Mean	Smooth-interface(in.xlb) Standard deviation	Rough-interface(in.xlb) Mean	Rough-interface(in.xlb) Standard deviation
12% No-Gap	70	0.1930	0.0904	0.1997	0.0893
	100	0.6823	0.2536	0.7066	0.2666
	130	1.7830	0.4745	1.8496	0.5376
	160	4.0750	1.2420	4.2433	1.4427
	190	10.7316	5.3607	11.9571	5.5182
Green	70	0.2727	0.2131	0.2607	0.1700
	100	1.3746	0.9002	1.4136	0.6137
	130	5.3375	3.3193	5.5044	1.8978
	160	16.6276	6.9595	18.7783	5.9661
	190	32.5559	6.8866	32.3969	6.4999
18% Gap	70	0.6742	0.1429	0.6460	0.1431
	100	1.7862	0.4382	1.6790	0.4711
	130	4.9285	1.7497	5.6610	2.9287
	160	15.1570	4.6211	17.3835	5.0875
	190	26.8885	3.9796	26.7100	3.4397
12% Gap	70	0.7493	0.1897	0.7797	0.2158
	100	1.6697	0.3801	1.6750	0.4198
	130	3.8950	1.2466	3.8402	1.1720
	160	13.1515	5.5661	13.8015	6.1471
	170	28.4590	5.8003	26.4441	7.1943
12% Cycling	70	0.1751	0.0661	0.2494	0.1956
	100	0.5870	0.1801	0.8282	0.5642
	130	1.6030	0.3905	2.0448	0.9689
	160	3.7612	0.9999	4.0389	1.8399
	190	12.0511	4.1576	12.882	7.0618

* Sample sizes are the same as in Table A1.

Table A4 : Statistics for total energy capacity per loop*.

Sample type	Load level(lb)	Smooth-interface(in.xlb) Mean	Smooth-interface(in.xlb) Standard deviation	Rough-interface(in.xlb) Mean	Rough-interface(in.xlb) Standard deviation
12% No-Gap	70	0.1087	0.0428	0.1131	0.0404
	100	0.3836	0.1554	0.4152	0.1591
	130	1.0608	0.3715	1.1955	0.4387
	160	2.7729	1.0322	3.2190	1.3063
	190	8.0227	4.3834	9.6003	4.5774
Green	70	0.1515	0.1223	0.1357	0.0761
	100	0.6932	0.5071	0.7230	0.3710
	130	2.9670	2.4358	3.0284	1.4685
	160	10.5079	5.5869	11.5427	4.3228
	190	23.5169	6.8348	22.8986	4.3898
18% Gap	70	0.6701	0.1412	0.6344	0.1437
	100	1.9938	0.4101	1.7770	0.4894
	130	5.2886	1.3097	5.5419	2.3802
	160	13.9497	3.3427	15.5567	4.0689
	190	25.8366	4.1114	25.5369	2.7568
12% Gap	70	0.7868	0.1818	0.8766	0.1788
	100	2.0373	0.4051	2.1861	0.4502
	130	4.7023	1.0457	4.9890	1.2150
	160	12.5013	3.7577	13.6762	4.5544
	190	26.0004	4.9156	25.0123	5.2854
12% Cycling	70	0.0917	0.0367	0.1242	0.0703
	100	0.2805	0.0999	0.4323	0.2793
	130	0.7767	0.2641	1.1533	0.6856
	160	2.0349	0.7797	2.9658	1.6416
	190	6.1783	3.1091	9.3340	6.1547

* Sample sizes are the same as in Table A1.

Table A5 : Statistics for damping ratio*.

Sample type	Load level(lb)	Smooth-interface Mean	Smooth-interface Standard deviation	Rough-interface Mean	Rough-interface Standsrd deviation
	70	0.2807	0.0508	0.2732	0.0534
12% No-	100	0.2867	0.0262	0.2732	0.0354
Gap	130	0.2744	0.0308	0.2548	0.0363
	160	0.2406	0.0324	0.2160	0.0317
	190	0.2199	0.0302	0.2002	0.0266
	70	0.2817	0.0534	0.2980	0.0712
Green	100	0.3266	0.0420	0.3174	0.0322
	130	0.3151	0.0467	0.3012	0.0364
	160	0.2688	0.0384	0.2653	0.0307
	190	0.2279	0.0318	0.2257	0.0179
	70	0.1635	0.0318	0.1653	0.0364
18% Gap	100	0.1441	0.0255	0.1569	0.0563
	130	0.1465	0.0260	0.1594	0.0338
	160	0.1712	0.0180	0.1771	0.0200
	190	0.1666	0.0128	0.1671	0.0188
	70	0.1588	0.0512	0.1429	0.0335
12% Gap	100	0.1342	0.0371	0.1225	0.0232
	130	0.1324	0.0287	0.1215	0.0165
	160	0.1635	0.0211	0.1554	0.0231
	190	0.1741	0.0103	0.1663	0.0178
	70	0.3293	0.1362	0.3016	0.0833
12%	100	0.3394	0.0585	0.3088	0.0458
Cycling	130	0.3370	0.0393	0.2981	0.0425
	160	0.3054	0.0379	0.2700	0.0471
	190	0.2693	0.0340	0.2394	0.0408

* Sample sizes are the same as in Table A1.

Table A6: Statistics for slip*.

Sample type	Load level (lb)N	Slip (in.) Tensile half-loops Mean	Tensile half-loops Standard deviation	Compression half-loops Mean	Compression half-loops Standard deviation
12% No-Gap	70 48	0.0017	0.0008	0.0015	0.0009
	100 49	0.0050	0.0020	0.0031	0.0019
	130 49	0.0111	0.0043	0.0064	0.0038
	160 49	0.0260	0.0128	0.0117	0.0064
	190 45	0.0689	0.0424	0.0242	0.0149
Green	70 40	0.0026	0.0019	0.0016	0.0013
	100 42	0.0095	0.0061	0.0048	0.0032
	130 40	0.0331	0.0253	0.0132	0.0077
	160 39	0.1006	0.0506	0.0381	0.0187
	190 36	0.1624	0.0439	0.0824	0.0330
18% Gap	70 23	0.0100	0.0025	0.0090	0.0022
	100 23	0.0207	0.0049	0.0173	0.0050
	130 24	0.0488	0.0225	0.0343	0.0113
	160 24	0.1126	0.0438	0.0703	0.0235
	190 21	0.1547	0.0383	0.1165	0.0277
12% Gap	70 23	0.0122	0.0026	0.0112	0.0028
	100 23	0.0223	0.0051	0.0195	0.0041
	130 23	0.0418	0.0123	0.0323	0.0070
	160 23	0.1025	0.0424	0.0601	0.0179
	190 20	0.1655	0.0410	0.1028	0.0334
12% Cycling	70 49	0.0011	0.0007	0.0018	0.0014
	100 49	0.0035	0.0017	0.0034	0.0036
	130 49	0.0080	0.0039	0.0067	0.0064
	160 47	0.0179	0.0102	0.0133	0.0117
	190 45	0.0527	0.0443	0.0294	0.0292

* Sample sizes are the same as in slip of tensile half-loops.

Table A7 : Statistics for energy*.

Sample type	Load level (lb)	Energy (in.xlb) absorbed per loop Mean	Energy (in.xlb) absorbed per loop Standard deviation	Energy (in.xlb) capacity per loop Mean	Energy (in.xlb) capacity per loop Standard deviation
12% No-Gap	70	0.1963	0.0890	0.1109	0.0412
	100	0.6952	0.2578	0.3997	0.1564
	130	1.1870	0.5035	1.1295	0.4087
	160	4.1609	1.3368	3.0005	1.1893
	190	11.3580	5.4152	8.8290	4.5036
Green	70	0.2658	0.1870	0.1425	0.0973
	100	1.3960	0.7472	0.7095	0.4324
	130	5.4334	2.5610	3.0023	1.9109
	160	17.8959	6.3934	11.1182	4.8379
	190	32.4720	6.5890	23.1906	5.6004
18% Gap	70	0.6619	0.1404	0.6546	0.1402
	100	1.7396	0.4455	1.8995	0.4492
	130	5.2643	2.3378	5.4047	1.8370
	160	16.1775	4.8661	14.6863	3.7009
	190	26.8205	3.6948	25.7224	3.5811
12% Gap	70	0.7651	0.1997	0.8337	0.1820
	100	1.6725	0.3922	2.1149	0.4263
	130	3.8664	1.1807	4.8519	1.1209
	160	13.4906	5.7520	13.1143	4.1412
	190	27.5525	6.3684	25.5558	4.9733
12% Cycling	70	0.2130	0.1504	0.1083	0.0582
	100	0.7101	0.4353	0.3580	0.2355
	130	1.8284	0.7696	0.9688	0.5520
	160	4.2094	1.5386	2.5102	1.3636
	190	11.4980	5.9357	7.8010	5.1055

* Sample sizes are the same as in Table A6.

Table A8 : Statistics for damping ratio*.

Sample type	Load level(lb)	Damping ratio	
		Mean	Standard deviation
12% No-Gap	70	0.2770	0.0517
	100	0.2798	0.0317
	130	0.2643	0.0348
	160	0.2280	0.0341
	190	0.2098	0.0298
Green	70	0.2911	0.0640
	100	0.3215	0.0368
	130	0.3071	0.0411
	160	0.2667	0.0336
	190	0.2268	0.0251
18% Gap	70	0.1643	0.0331
	100	0.1497	0.0411
	130	0.1524	0.0299
	160	0.1739	0.0188
	190	0.1668	0.0149
12% Gap	70	0.1505	0.0427
	100	0.1281	0.0305
	130	0.1267	0.0233
	160	0.1593	0.0221
	190	0.1706	0.0143
12% Cycling	70	0.3151	0.1120
	100	0.3237	0.054
	130	0.3172	0.0451
	160	0.2873	0.0460
	190	0.2540	0.0402

* Sample sizes are the same as in Table A6.

APPENDIX B

PROPERTIES AND MC OF MATERIALS

Table B1: Statistics for MC of stud and plywood sections.

	Sample type*			
	12% No-Gap	Green	12% Gap	12% Cycling
Stud section				
Mean	12.6	157.4	13.6	14.6
Standard deviation	0.562	0.756	0.338	0.321
Plywood section				
For joints with smooth interface				
Mean	9.7	9.5	9.2	11.4
Standard deviation	0.886	0.708	0.405	0.755
For joints with rough interface				
Mean	10.0	9.4	10.0	9.9
Standard deviation	0.500	0.732	0.478	1.980

* No MC measurement for 18% Gap Sample.

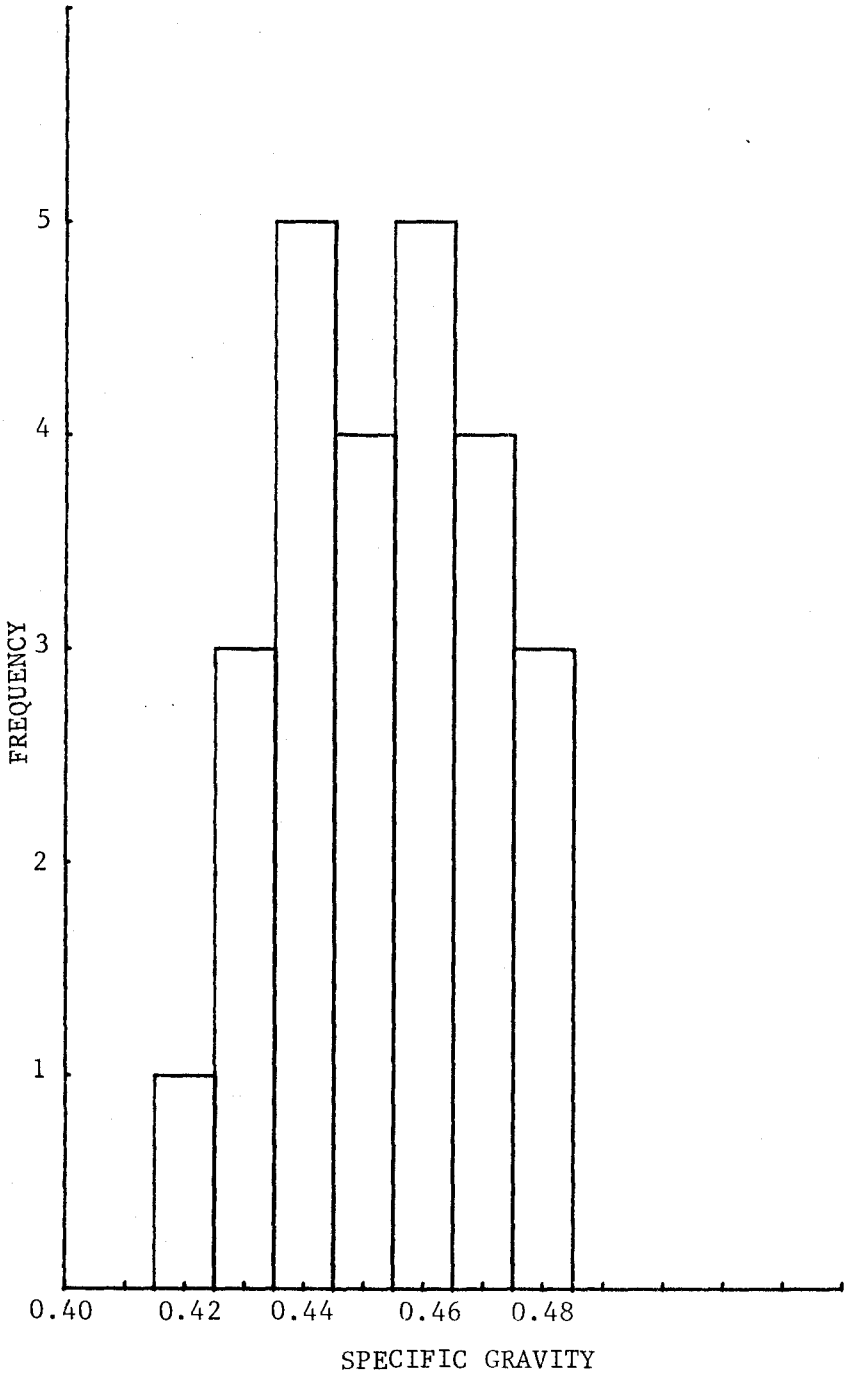

Histogram of Douglas-fir stud specific gravity.

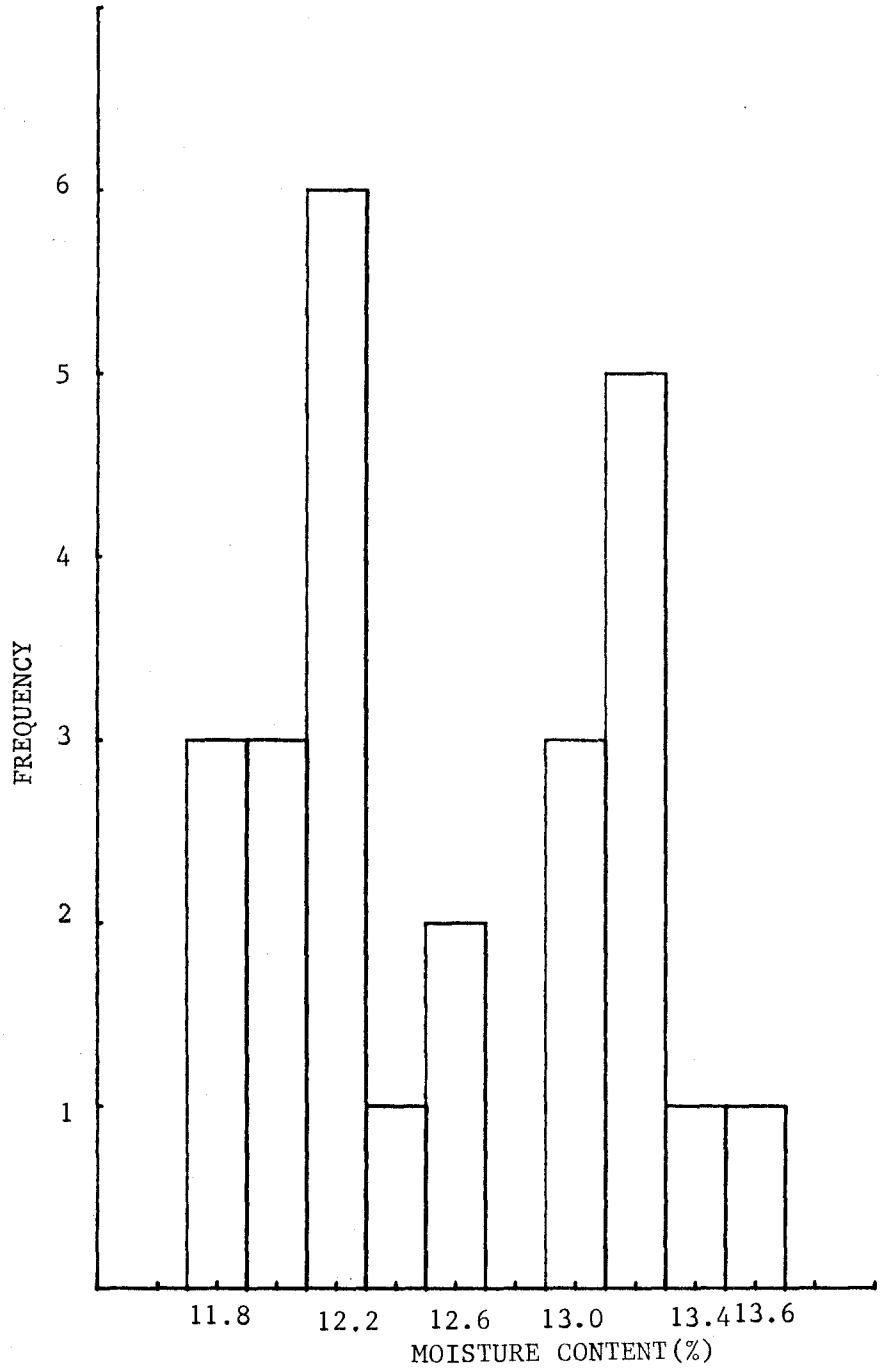

Histogram of stud moisture content in 12% No-Gap Sample.

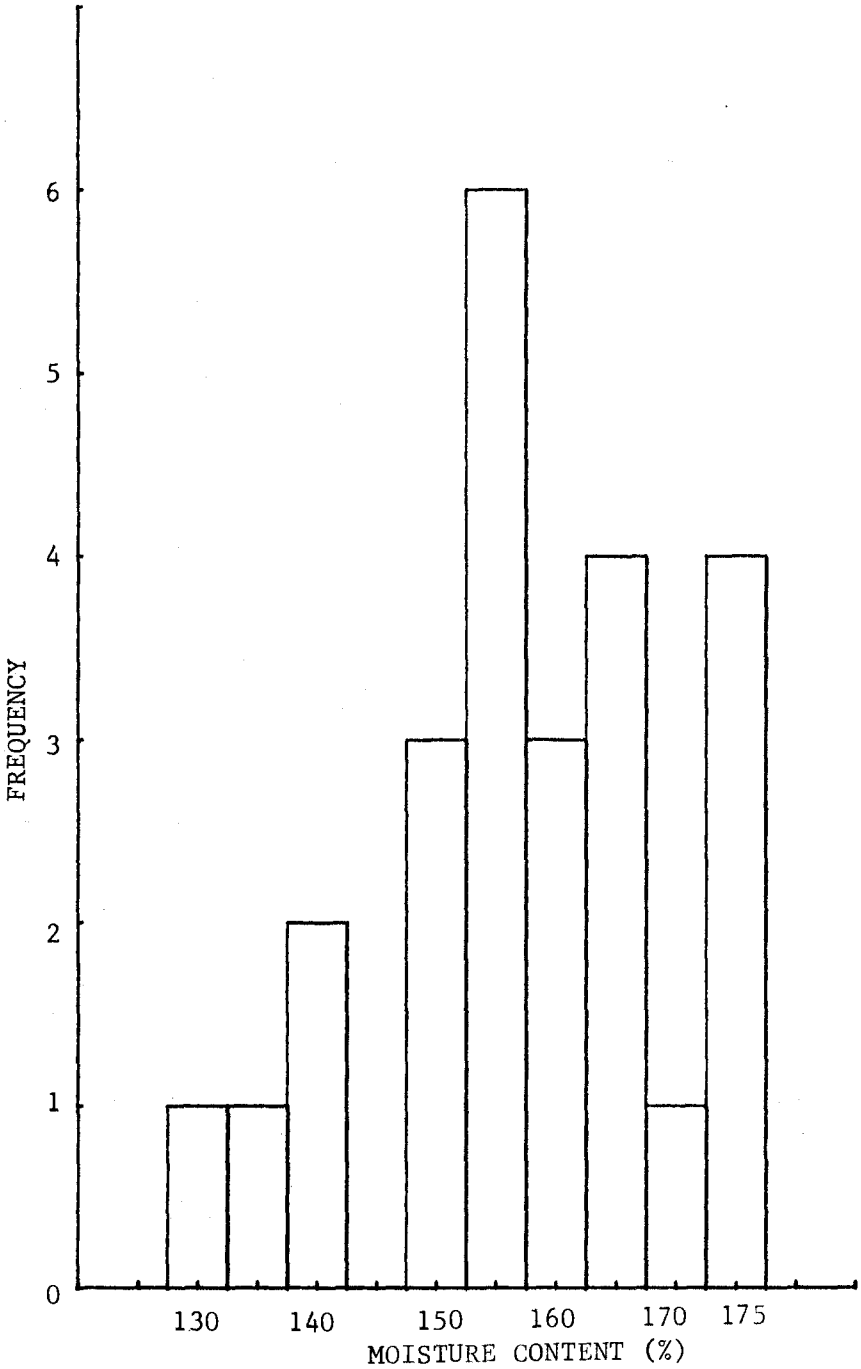

Histogram of stud moisture content in Green Sample.

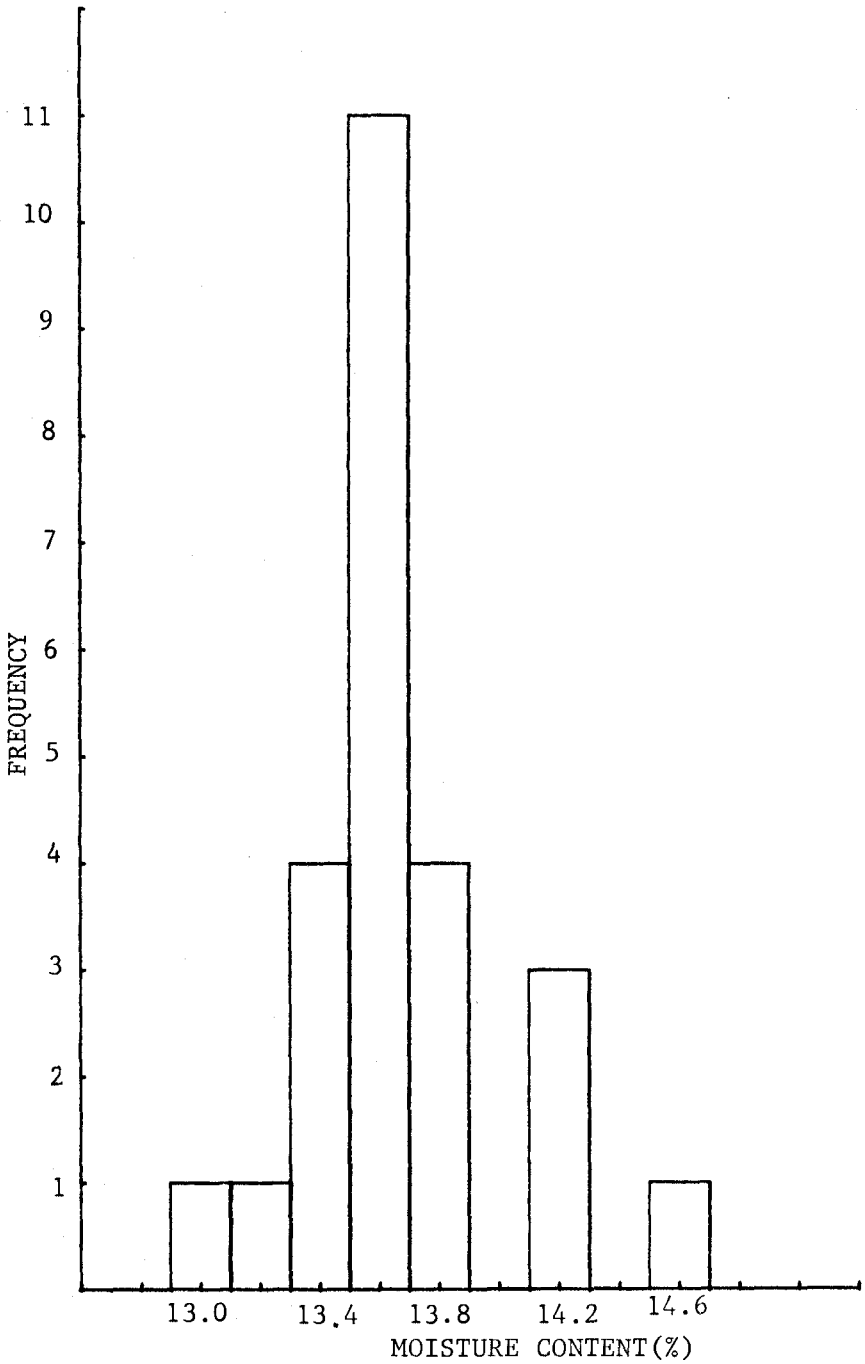

Histogram of stud moisture content in 12% Gap sample.

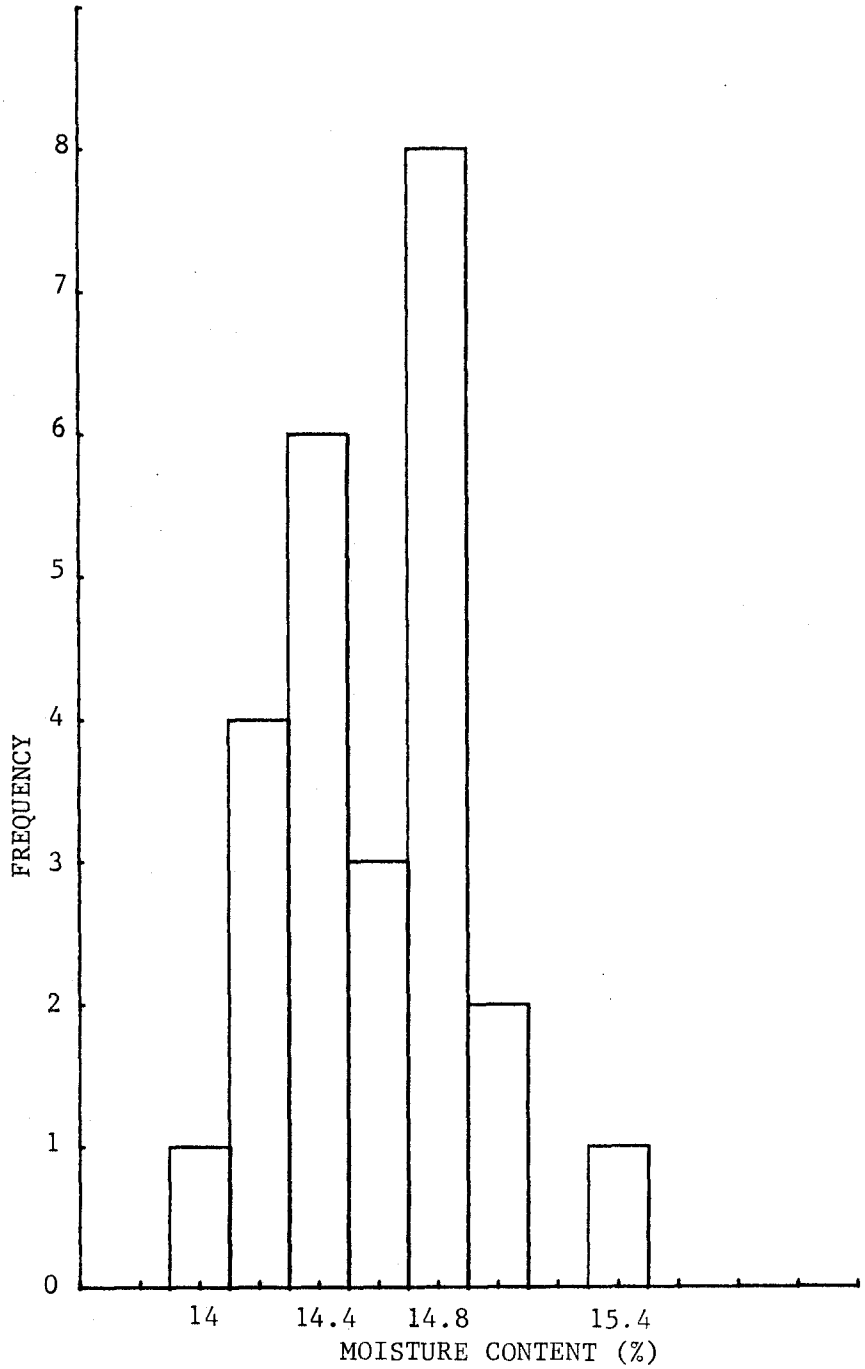

Histogram of stud moisture content in 12% Cycling Sample.

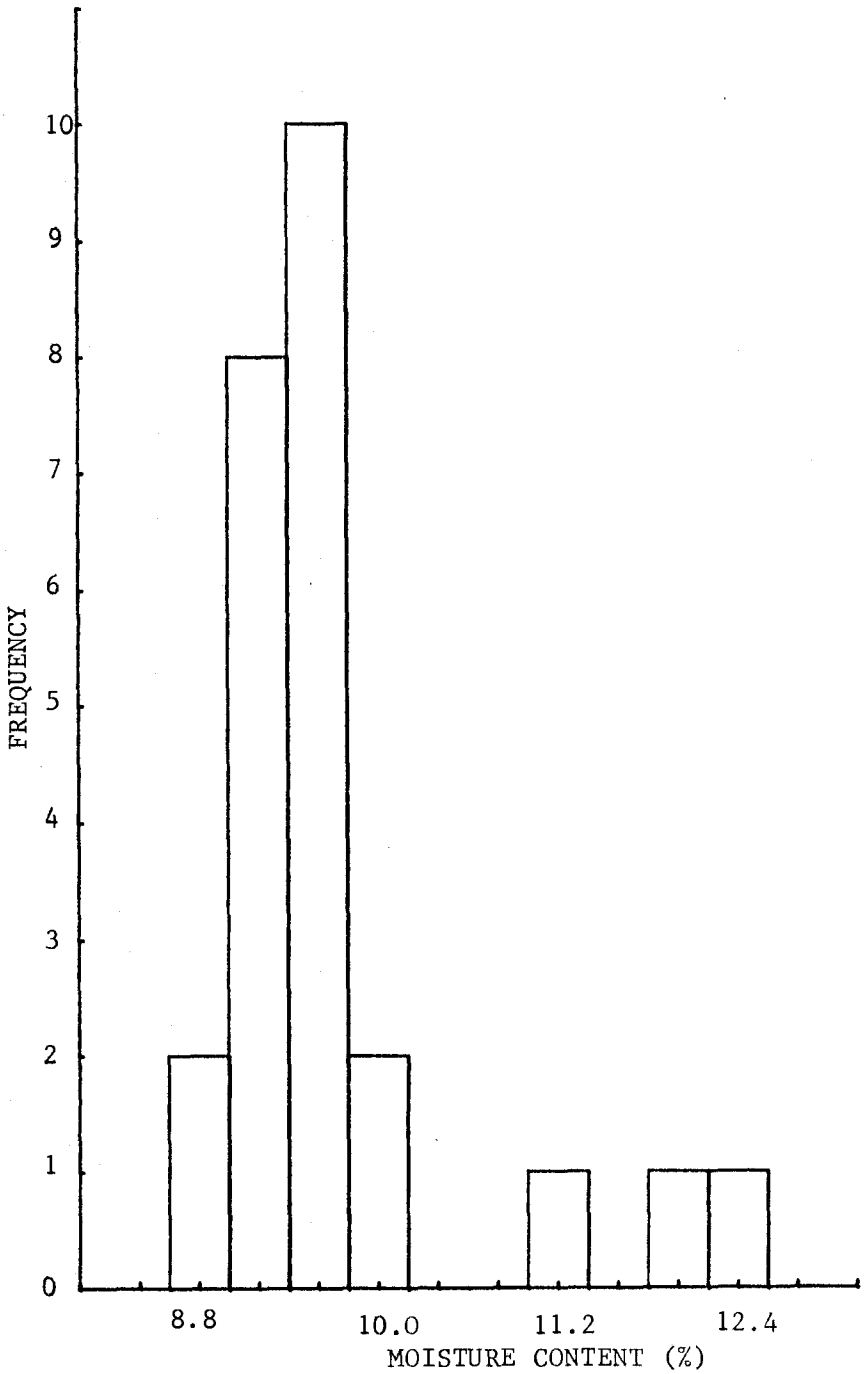

Histogram of plywood moisture content in 12% No-Gap Sample used with smooth-interface joints.

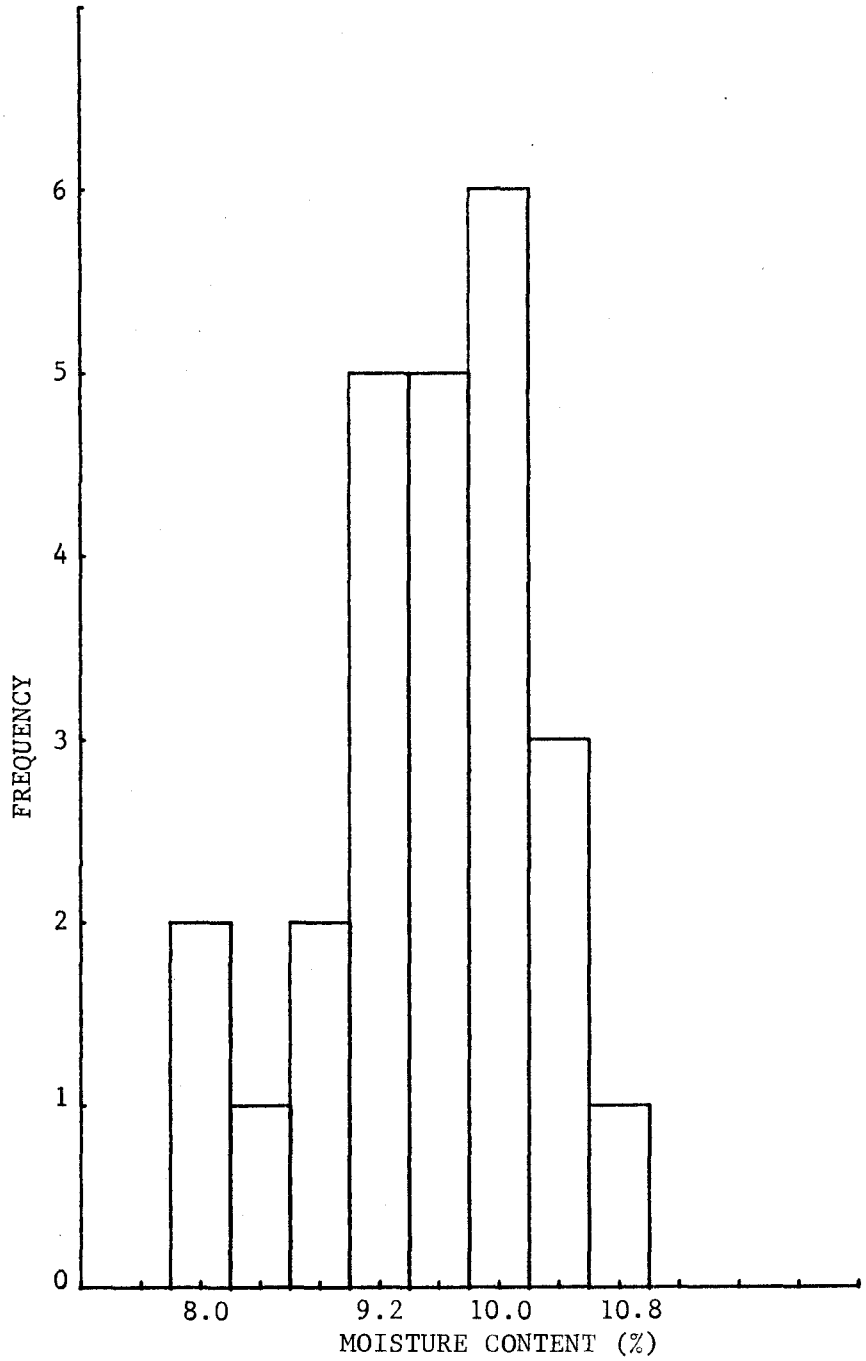

Histogram of plywood moisture content in Green Sample used with smooth-interface joints.

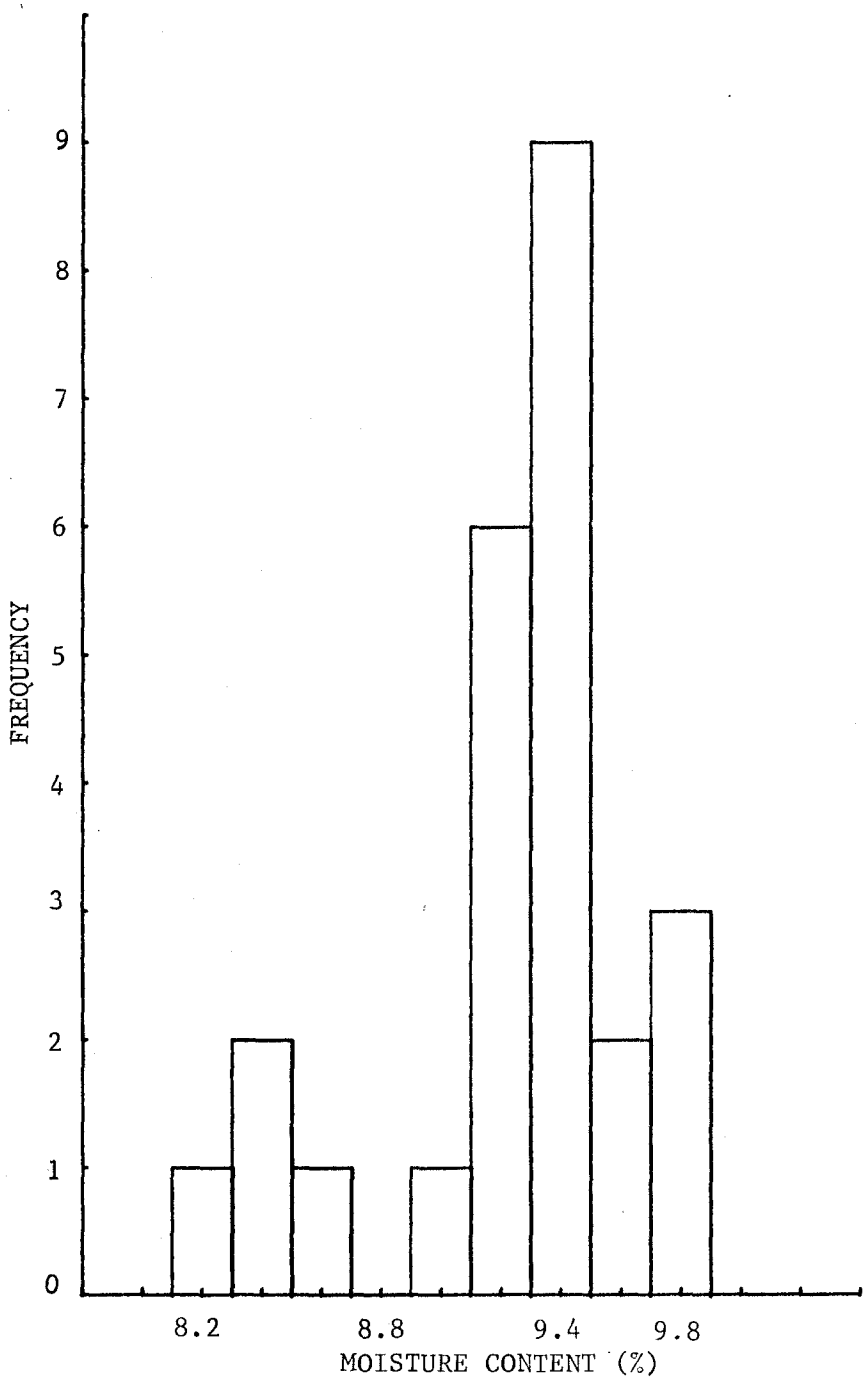

Histogram of plywood moisture content in 12% Gap Sample used with smooth-interface joints.

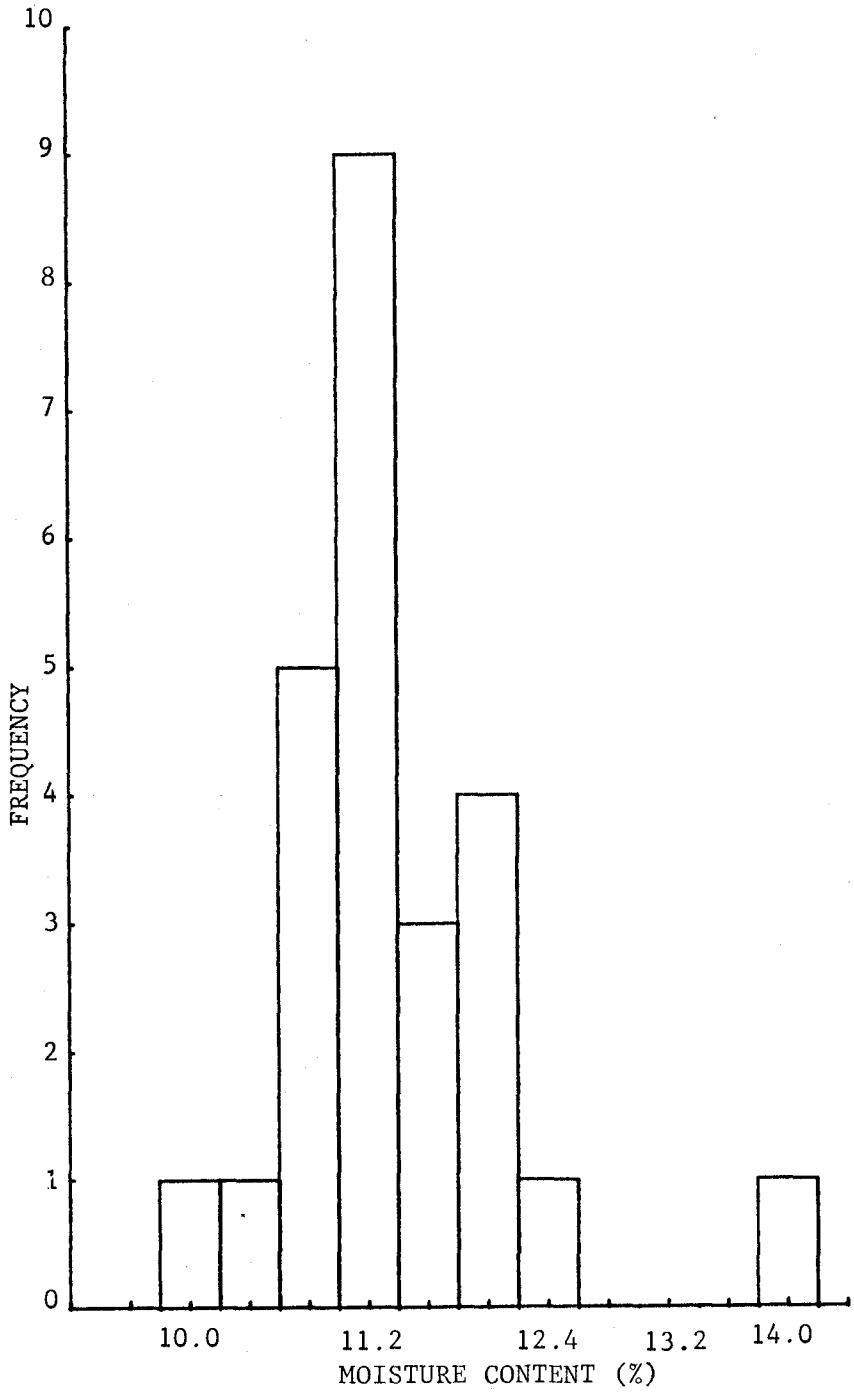

Histogram of plywood moisture content in 12% Cycling Sample used with smooth-interface joints.

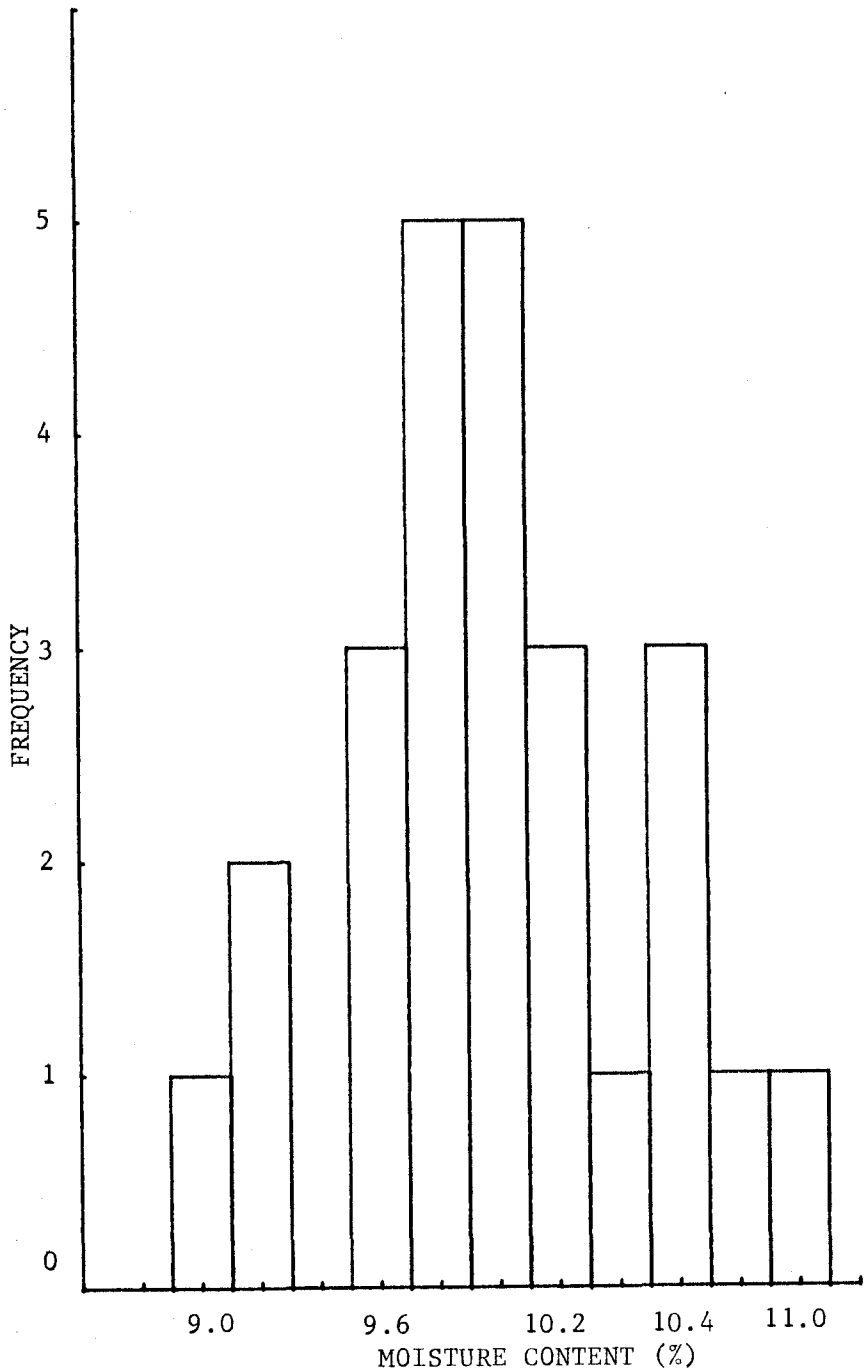

Histogram of plywood moisture content in 12% No-Gap Sample used with rough-interface joints.

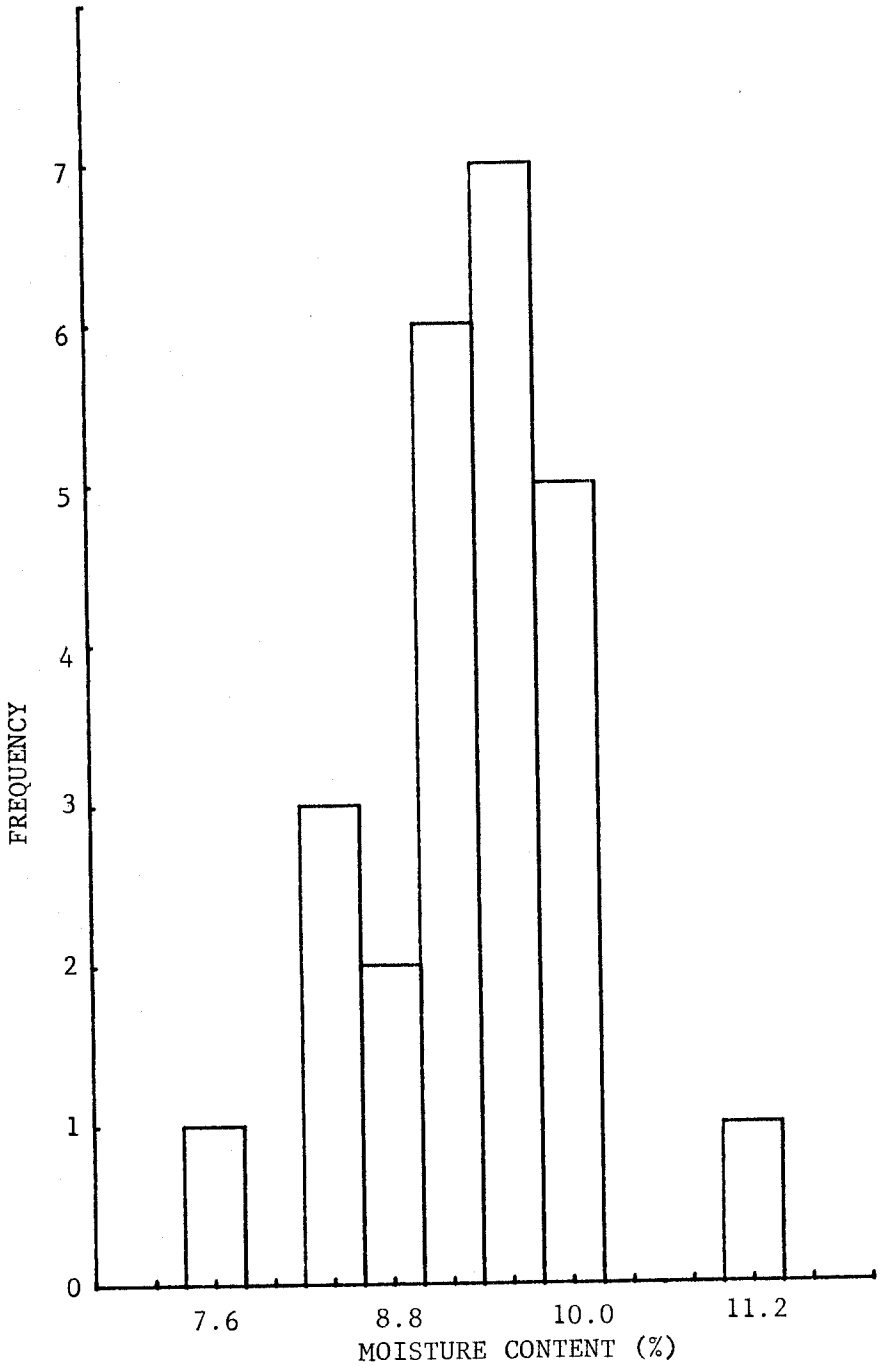

Histogram of plywood moisture content in Green Sample used with rough-interface joints.

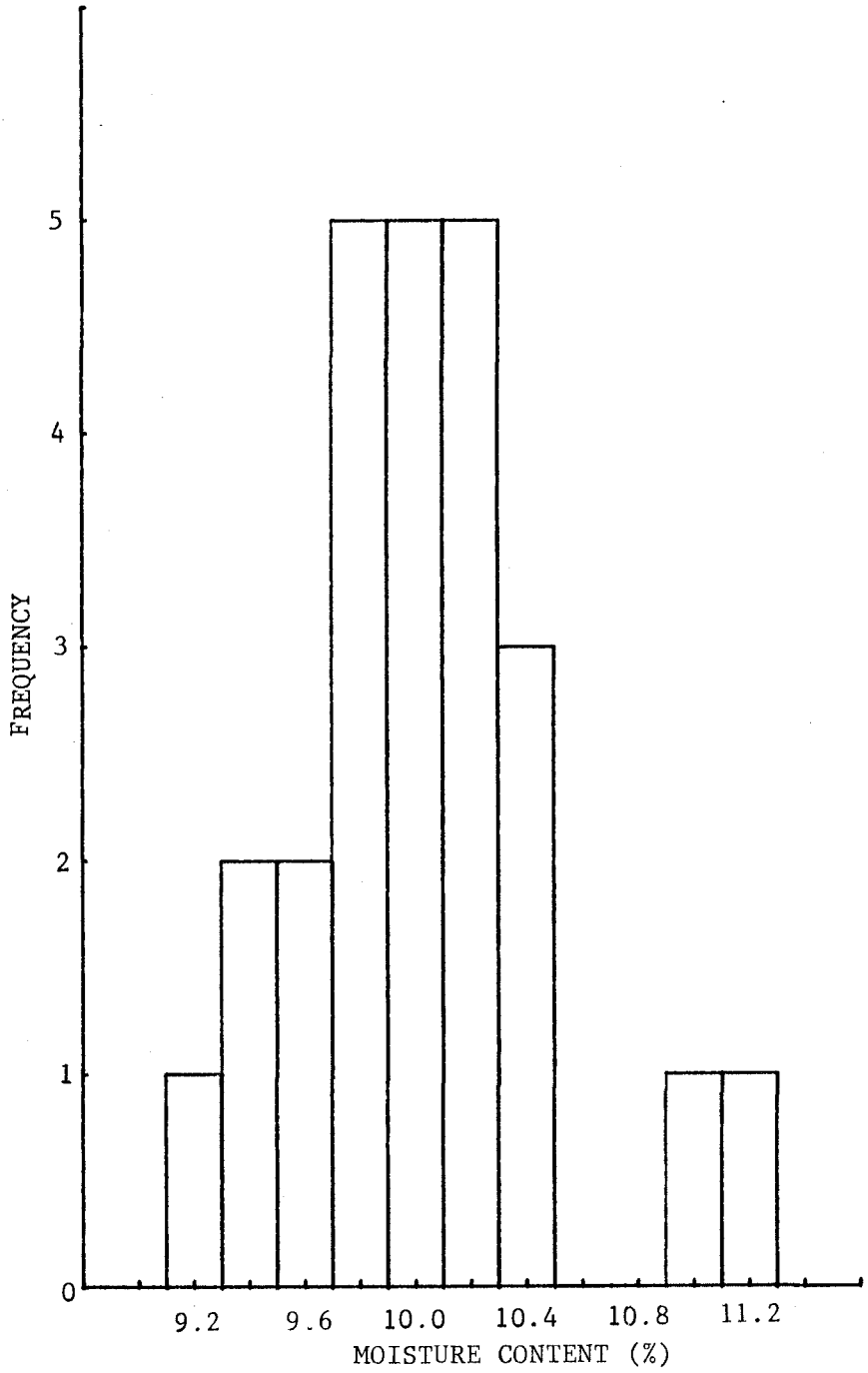

Histogram of plywood moisture content in 12% Gap Sample used with rough-interface joints.

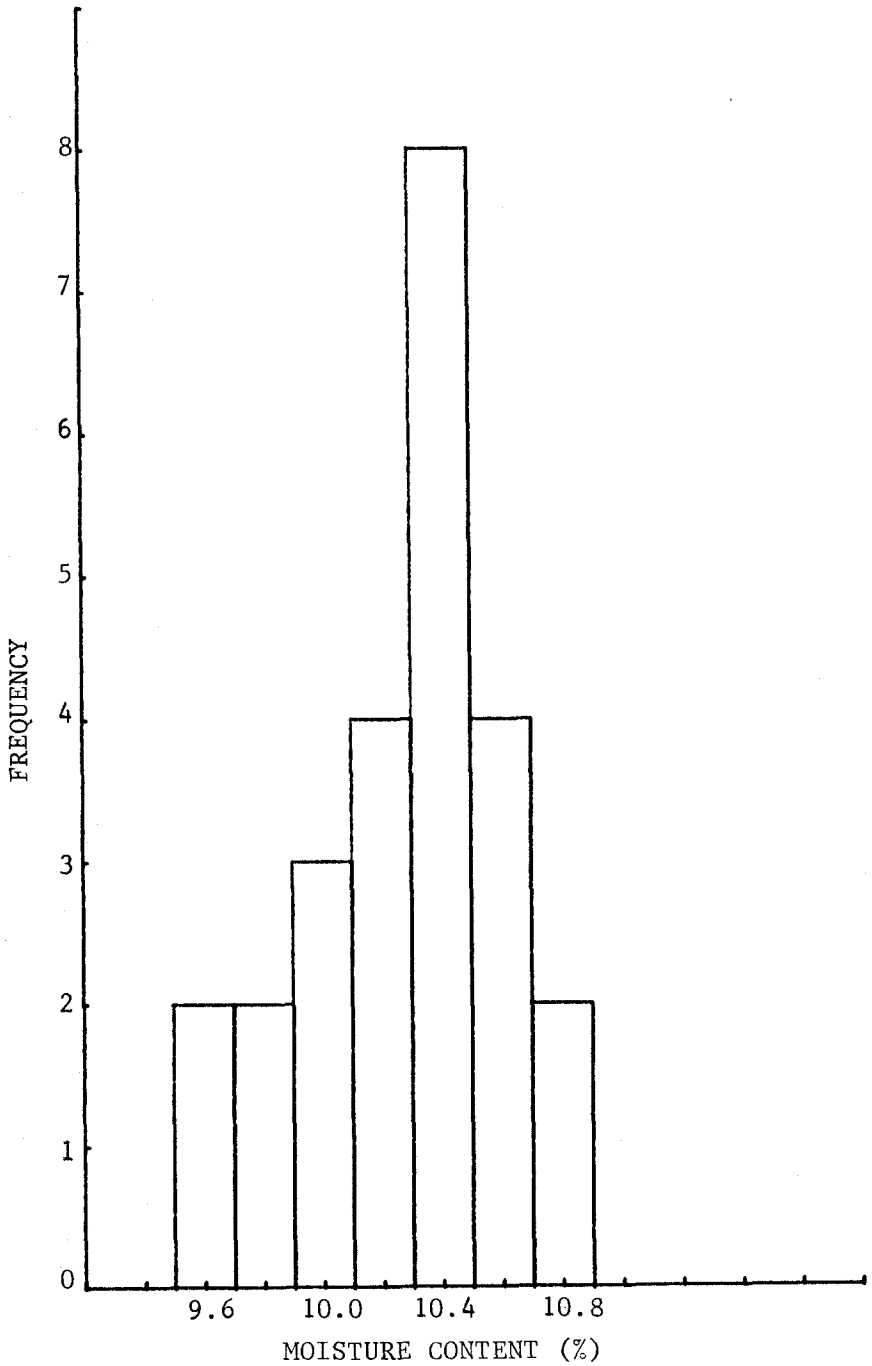

Histogram of plywood moisture content in 12% Cycling Sample used with rough-interface joints.